# Evaluating the role of coastal hypoxia on the transient expansion of microencruster intervals during the early Aptian

ALEXANDER HUETER ⬩, STEFAN HUCK, ULRICH HEIMHOFER, STÉPHANE BODIN, STEFAN WEYER, KLAUS P. JOCHUM ⬩, YVONNE ROEBBERT AND ADRIAN IMMENHAUSER

## LETHAIA

Worldwide, a growing number of modern coastal marine ecosystems are increasingly exposed to suboxic- or even anoxic conditions. Low seawater oxygen levels trigger significant ecosystem changes and may result in mass mortality of oxygen-sensitive biota. The applicability of observations from recent (anthropogenically influenced) suboxic coastal settings to fossil anoxic shallow-marine environments is, however, as yet poorly explored. The test case documented here are upper Barremian to lower Aptian strata in the Lusitanian Basin (Ericeira section, Portugal). These are characterized by the transient demise of rudist–coral communities and the rapid establishment of microencruster facies in the vacant ecological niches. The hypothesis is tested that the temporal expansion of the microencrusting organism *Lithocodium aggregatum* took place in response to platform-top seawater oxygen depletion. We critically discuss the outcome of a multi-proxy palaeoseawater redox approach (e.g. Rare Earth Elements (REEs), U isotopes and palaeoecology) and put the robustness of the proxies applied here to the test. This is done by considering issues with these methods in general but also emphasizing the significance of terrigenous contamination and fractionation effects. Data shown here document that evidence for coastal seawater oxygen depletion in the prelude of Oceanic Anoxic Event (OAE) 1a is lacking, and hence, anoxia was not the driving mechanism for the demise of rudist–coral ecosystems in the proto-North Atlantic platform setting studied here. In contrast, well-oxygenated early Aptian platform-top water masses are proposed for this site. Geologically short (decades to millennia) fluctuations in seawater oxygen levels cannot be excluded, however. But even if these took place, they offer no explanation for the Kyr to Myr-scale patterns discussed here. The present paper is relevant as it sheds light on the complexity of mechanisms that drive punctuated Early Cretaceous coral–rudist ecosystem turnover, and assess strengths and weaknesses of redox proxies applied to ancient shallow-marine platform carbonates. □ *Anoxia, cerium anomalies, Cretaceous, Oceanic Anoxic Event 1a, redox proxies, uranium isotopes.*

*Alexander Hueter ✉ [alexander.hueter@rub.de], and Adrian Immenhauser [Adrian.immenhauser@rub.de], Institute for Geology, Mineralogy and Geophysics, Sediment and Isotope Geology, Ruhr-University Bochum, Bochum 44801, Germany; Stefan Huck [huck@geowi.uni-hannover.de], Ulrich Heimhofer [heimhofer@geowi.uni-hannover.de], Institute for Geology, Leibniz University Hannover, Hannover 30167, Germany; Stéphane Bodin [stephane.bodin@geo.au.dk], Department of Geoscience, Aarhus University, Aarhus 8000, Denmark; Stefan Weyer [s.weyer@mineralogie.uni-hannover.de], Yvonne Roebbert [y.roebbert@mineralogie.uni-hannover.de], Institute for Mineralogy, Leibniz University Hannover, Hannover 30167, Germany; Klaus P. Jochum [k.jochum@mpic.de], Climate Geochemistry Department, Max Planck Institute for Chemistry, Mainz 55128, Germany; manuscript received on 19/02/2020; manuscript accepted on 26/09/2020.*

Oxygen is a key element for the metabolism of most marine organisms. Seawater oxygen depletion is a threat, particularly to shallow coastal areas, and indeed, the number of seasonal to permanent oxygen-depleted coasts has dramatically increased during the past 50 years (Diaz & Rosenberg 2008). The growing number of coastal hypoxic ecosystems is linked to higher rates of anthropogenic nutrient input, enhanced organic matter production and eutrophication (Rabalais *et al.* 2010). Hypoxia has a variety of effects on population structure and community composition (Rabalais & Turner 2001; Levin *et al.* 2009). Severe hypoxia can culminate in the creation of 'dead zones' (Rabalais *et al.* 2010) and mass mortality of many marine species. Nevertheless, organism responses differ among taxa, depending on the duration and degree of oxygen depletion (Rabalais & Turner 2001) and the mobility of the organism considered. Further, independent of the recently observed anthropogenic patterns, seawater hypoxia

or even anoxia are well-known phenomena throughout Earth's history (Schlanger & Jenkyns 1976; Jenkyns 2010; Rabalais *et al.* 2010; Dickson *et al.* 2012).

The most severe and globally traceable anoxic events are referred to as Oceanic Anoxic Events (OAEs), the early Aptian OAE 1a being one of the most prominent examples (Coccioni *et al.* 1987; Jenkyns 2010). Oceanic Anoxic Events are often accompanied by major geochemical changes in the water column (Jenkyns 2010) and changes in both, shallow-water ecosystems (Weissert *et al.* 1998; Föllmi *et al.* 2006, 2007; Hueter *et al.* 2019) and pelagic planktonic and benthic biota assemblages (Erba *et al.* 2010; Bottini *et al.* 2012; Robinson *et al.* 2017). Potential reasons for such ecosystem changes include eutrophication, high sea-surface temperatures, sea-level rise, low seawater pH (acidification) or elevated seawater salinity (Hart *et al.* 2003; Nielsen *et al.* 2003; Smith *et al.* 2006; Guinotte & Fabry 2008; Chen 2008; Kirwan *et al.* 2010).

Previous work (Immenhauser *et al.* 2005; Föllmi *et al.* 2006, 2012; Waite *et al.* 2007; Burla *et al.* 2008; Rameil *et al.* 2010; Huck *et al.* 2010, 2011, 2012, 2013; Bover-Arnal *et al.* 2011) has reported on a significant Aptian biological turnover in shallow-water settings across the Tethyan realm. The general pattern observed is that a diverse marine fauna of rudist bivalves, corals, benthic foraminifera, gastropods and echinoderms is temporarily replaced by taxonomically poorly constrained microencrusting organisms, including *Lithocodium aggregatum* (filamentous-septate heterotrichale ulvophycean alga; Schlagintweit *et al.* 2010) and *Bacinella irregularis* (purely euendolithic ulvophycean alga; Schlagintweit *et al.* 2010). In contrast with the northern Tethys, characterized by episodes of platform drowning, *L. aggregatum* and *B. irregularis* drive carbonate production in the proto-North Atlantic domain (Huck *et al.* 2012). Following previous workers (Leinfelder *et al.* 1993; Rameil *et al.* 2010), we argue that these microencruster communities, similar to many modern marine organisms (Diaz & Rosenberg 1995; Altieri & Diaz 2019), were significantly more tolerant with regard to environmental stressors including low dissolved seawater oxygen levels compared to coral–rudist ecosystems.

The approach followed here applies tools and concepts recently tested in the Central Tethyan realm (Kanfanar section, Croatia; Hueter *et al.* 2019). These tools include detailed fieldwork, carbonate microfacies analysis and SEM analysis, but also involve state-of-the-art geochemical seawater redox proxies such as cerium (Ce) anomalies and uranium (U) isotope ratios. By applying these tools, we intend to critically test their robustness with regard to potential near-coastal terrigenous contamination and/or fractionation effects. In the Central Tethys, transient stages of platform-top hypoxia have been shown to act as main driving mechanism for rudist–coral decline and microencruster expansion. There, these events are coeval with OAE 1a and related organic-rich pelagic deposits (black shales) documenting basinal anoxia (Hueter *et al.* 2019). This is of relevance for the proto-North Atlantic case example tested here, as lower Aptian shallow-water limestones of the Lusitanian Basin (Portugal) were deposited prior to the onset of OAE 1a (Heimhofer *et al.* 2007; Burla *et al.* 2008; Huck *et al.* 2012) but show microencruster intervals (correlated between the Ericeira, Cresmina and Sao Juliao sections) comparable to those in the Central Tethyan realm.

Having established the relation between microencruster facies and syn-OAE 1a platform-top seawater oxygen depletion for the Central Tethyan realm (Hueter *et al.* 2019), the research question raised here is, if the decline of coral–rudist assemblages and the coeval mass occurrence of these microencrusters in these proto-Atlantic sections represent a more general, palaeoecological pattern that can be linked to low seawater dissolved oxygen levels in general? Moreover, if the hypothesis 'microencruster blooms are a proxy for platform-top anoxia' holds true, then the Portugal section would provide evidence that, at least in some regions, low dissolved seawater oxygen levels established prior to OAE 1a.

## Geological setting

During the Early Cretaceous, the Lusitanian Basin was located along the western Iberian margin at a palaeolatitude of 25 to 30° North (van Hinsbergen *et al.* 2015). At this time, the tectonic regime changed from rifting to drifting and the shelf areas were affected by local subsidence (Hiscott *et al.* 1990; Rasmussen *et al.* 1998), resulting in flooding of the basin during Barremian–Aptian times (Wilson *et al.* 1989; Dinis *et al.* 2008).

The studied coastal Ericeira outcrop is located north of Lisbon (38°57′39.62″N/9°25′11.16″W), in the centre of the town of Ericeira (Fig. 1A, B). The Ericeira section is built by ~60 m of mixed carbonate–siliciclastic sedimentary rocks of late Barremian to early Aptian age (Burla *et al.* 2008). Three lithostratigraphical units can be distinguished: the Regatão, the Cresmina and the Rodízio formations (Rey *et al.* 2003). The Cresmina Formation is subdivided into Cobre, Ponta Alta and Praia da Lagoa Members. The mixed carbonate–siliciclastic deposits of the Cobre Member (Barremian) are overlain by thickly bedded

rudist-bearing carbonates of the Ponta Alta Member (Aptian), composed of massive grainstone beds with numerous rudist bivalves, nerinid gastropods, madreporid corals and abundant *L. aggregatum* facies.

The *Lithocodium*-bearing interval of the Ponta Alta Member was studied in great detail and is composed of oncoidal floatstones, columnar-patchy boundstones and a prominent, 0.4 m thick *L. aggregatum* patch reef facies (see 'pinnacle interval' of Huck *et al.* 2012). The latter grade laterally into fine-grained, quartz-rich, orbitolinid grain- to pack-stones and marls. The stratigraphically overlying Praia da Lagoa Member is composed of orbitolinid-rich, oyster-bearing marls and limestones, characterizing a protected lagoonal setting (Rey *et al.* 2003; Dinis *et al.* 2008; Huck *et al.* 2014). Above, the Praia da Lagoa Member is unconformably overlain by coarse-grained siliciclastics of the Rodízio Formation, marking the transition towards continental conditions.

Based on observations of palynomorphs (Heimhofer *et al.* 2007), rudists and orbitolinids (Masse & Chartrousse 1997; Skelton & Masse 1998; Burla *et al.* 2008), the Ericeira section has been assigned to the early Aptian. This result is supported by carbon- and strontium-isotope chemostratigraphy (Burla *et al.* 2008; Burla *et al.* 2009; Huck *et al.* 2012). The nanno-fossil biostratigraphy of Da Gama *et al.* (2009) supports an early Aptian age for the Ponta Alta Member as well but suggests a late Aptian age for the unconformably overlying Praia da Lagoa Member.

# Methods

## Fieldwork and thin-section microscopy

Although our study builds on the data foundation published in Huck *et al.* (2012), we have significantly refined the sampling and data framework. Hence, a detailed lithological log of the key interval of the stratigraphical section was generated (Fig. 2). Eleven samples (ER1 to ER11; Fig. 3) were studied with the aim to identify changes in the biotic composition and to obtain the best possible material for geochemical analysis.

Stratigraphical intervals characterized by normal marine biota composition (corals, rudists, echinoderms, gastropods) were separated from intervals yielding the abundant (partly rock-forming) microencruster facies that potentially signifies lowered seawater oxygen levels (Fig. 3). By means of thin-section analysis, skeletal components were assessed for their frequency distribution in a semi-quantitative manner applying the following nomenclature: 1, very abundant; 2, abundant; 3, rare; 4, very rare; and 5, absent, in order to describe the relative volumetric significance of different components. Special focus was on the presence of *L. aggregatum* and its corresponding growth forms. For a discussion on the taxonomy of this organism, the reader is referred to Schlagintweit *et al.* (2010). For reasons of simplicity, we refer to *L. aggregatum* dominated carbonates as 'microencruster' facies throughout this study.
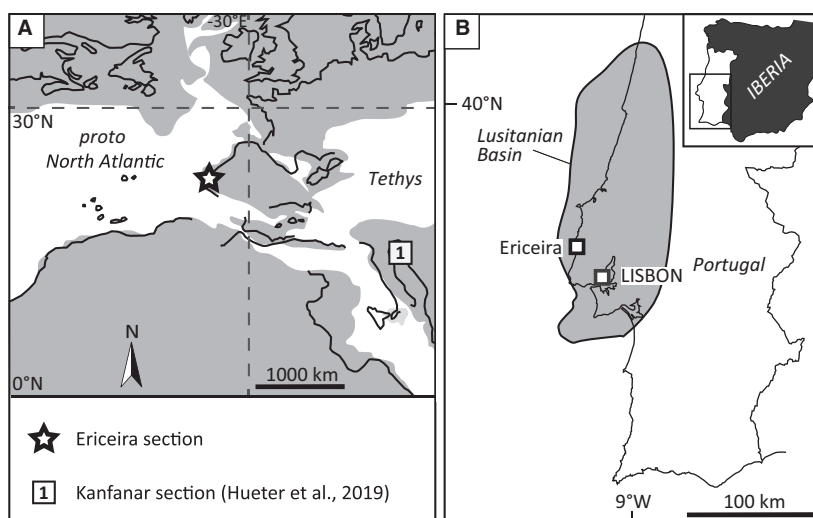


-*Fig. 1.* A, palaeogeographical reconstruction of the western Northern Hemisphere during the late Early Cretaceous (Barremian–Aptian boundary; 125 ± 1.0 Ma), modified after Hay *et al.* (1999) and Huck *et al.* (2012). The Ericeira study site in western Portugal is marked by an asterisk. B, map of Portugal showing the location of the study area in the Lusitanian Basin with location of the Ericeira section in the vicinity of Lisbon (modified after Alves *et al.*2009).
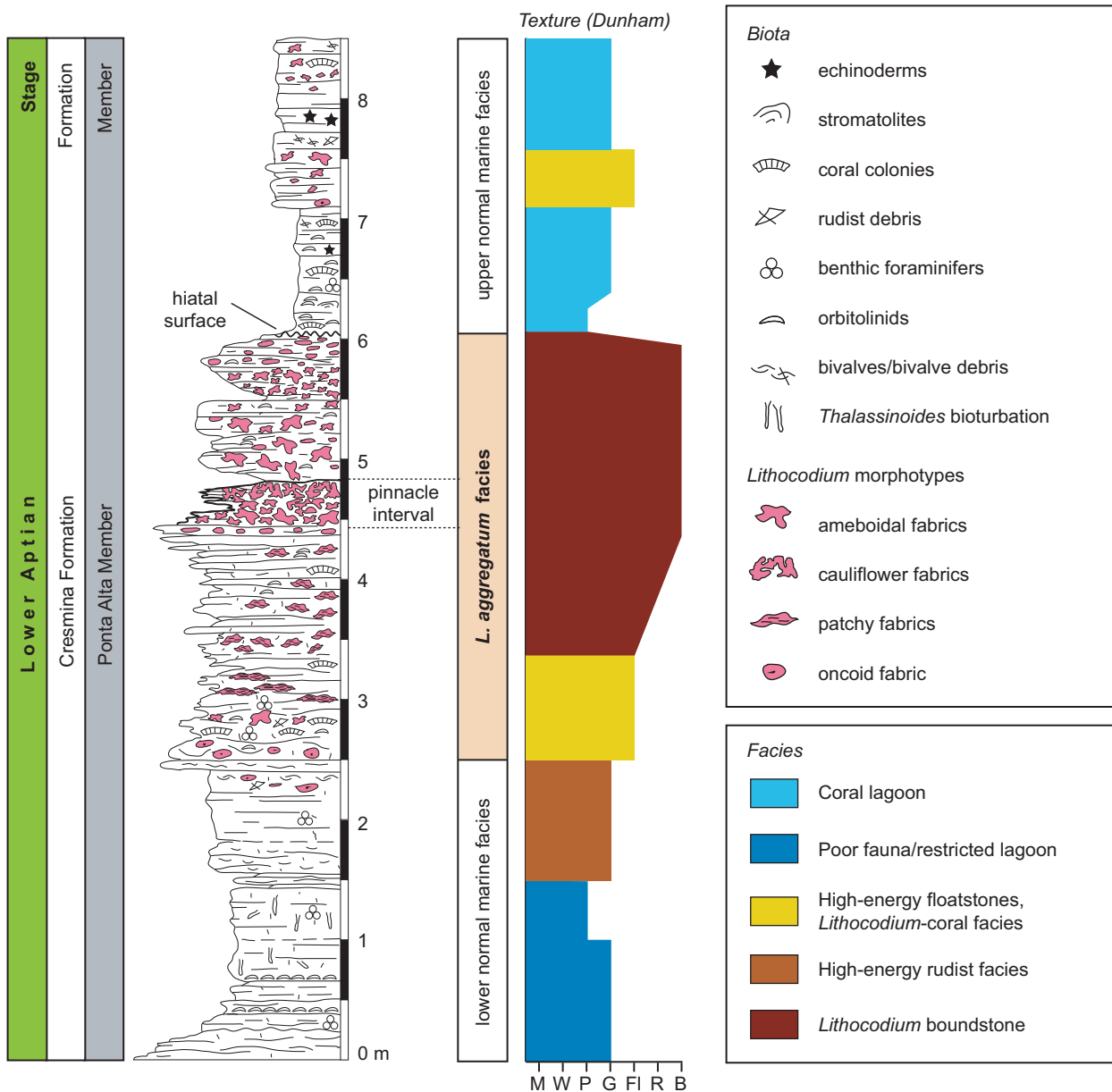
*Fig. 2.* Lithostratigraphy, erosional profile with biota distribution and texture/facies plotted against stratigraphical thickness (m) of the Ericeira section, Lusitanian Basin, Portugal.

## Scanning electron microscopy

A total of six samples were examined using a high-resolution field emission scanning electron microscope (HR-FESEM type Zeiss Merlin Gemini 2) with a high electrical voltage of 5–10 kV at RUB. Prior, samples were cut into small cubes, glued onto glass slides and coated with gold. The freshly broken surface facing towards the top was analysed with scanning electron microscopy (SEM) and energy-dispersive X-ray spectroscopy (EDS) in order to detect indication for diagenetic overprint. Furthermore, we aimed to identify microbially mediated

automicrite (terminology *sensu* Neuweiler & Reitner 1992), because the geochemical palaeoredox analyses performed here require significant portions of *in situ* deposited fine-grained carbonates (0.5–1 g).

## Geochemical methods

For 'Laser Ablation-Inductively Coupled Plasma-Mass Spectrometry' (LA-ICP-MS), thick sections were prepared at RUB. Rock samples were examined with a magnifying glass, and a suitable part was marked for further preparation. They were then sawn into small blocks, in order to generate glass pellets
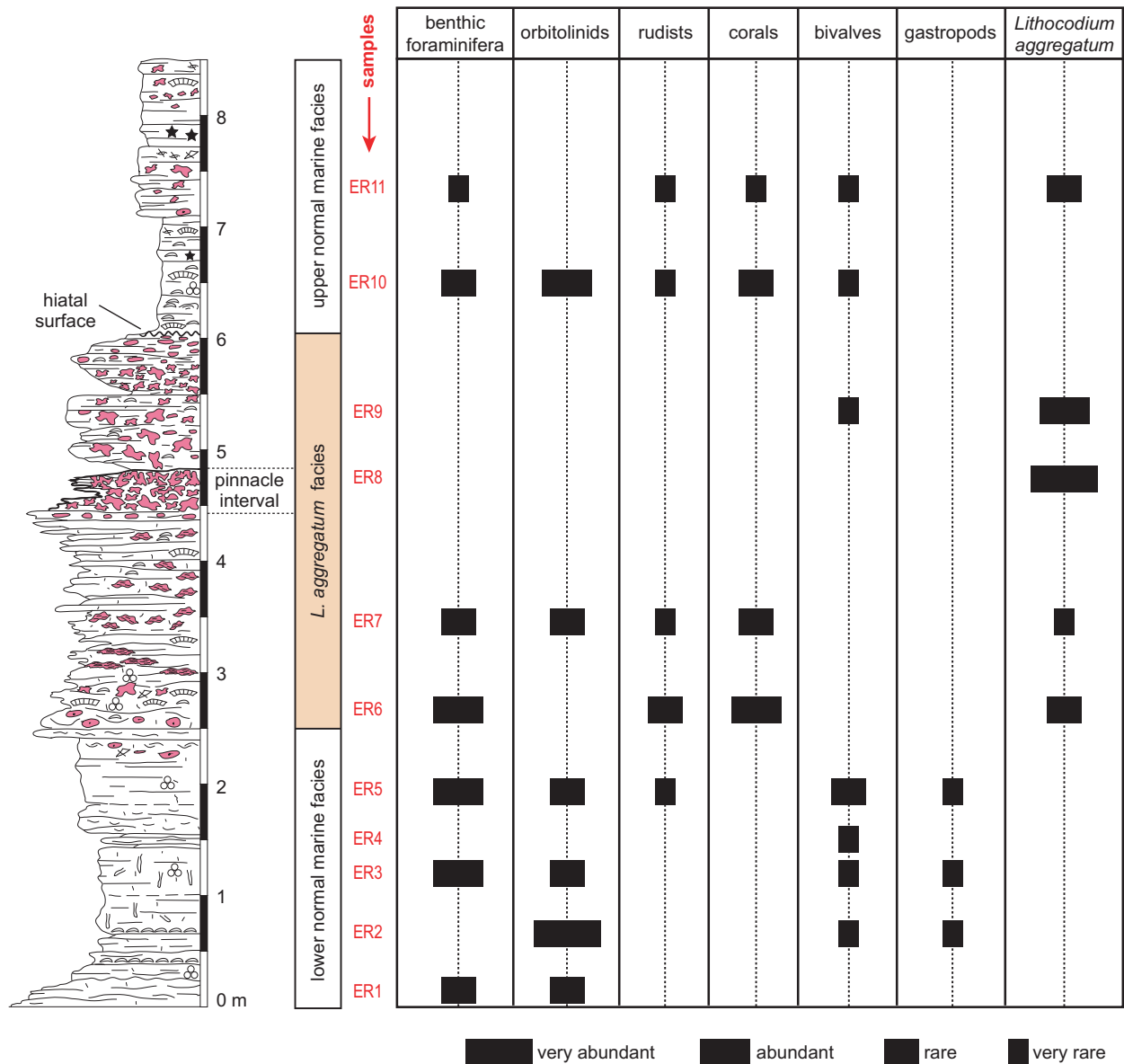
*Fig. 3.* Stratigraphical distribution patterns of biota assemblages of the Ericeira section for selected groups of organisms including benthic foraminifers, orbitolinids, rudists, corals, bivalves, gastropods, and the microencrusting organism *Lithocodium aggregatum*. Bar thickness corresponds to semi-quantitative abundance of specific organism groups as based on thin-section analysis.

for LA-ICP-MS analyses. Analysis were performed on eleven samples with a 213 nm, Q-switched, Nd: YAG laser from New Wave, connected to a Thermo Finnigan ELEMENT2 sector field (SF) ICP-MS located at the Max Planck Institute for Chemistry in Mainz, Germany. The main focus of the analysis was on obtaining data for the calculation of the cerium anomaly (Ce/Ce*). The Ce/Ce* ratio is used as a proxy for the degree of seawater oxygenation (Tostevin *et al.* 2016). Measurements include Rare Earth Elements (REEs) and redox-sensitive trace elements. Every sample was measured at three spots distributed over two different portions of the thick sections.

Standard settings of the laser system were the following: (1) an energy density of 7 J/cm$^2$; (2) a pulse rate of 10 Hz; (3) the instrument was tuned to achieve low oxide production rates (ThO/Th < 0.5 %); (4) laser spot diameter size of 60 – 120 μm; and (5) wash out, blank count rate and ablation times of 45 s, 20 s and 110 s, respectively. We used NIST-612 and MACS-3 for external standardization and $^{43}$Ca as an internal standard, to calculate absolute element concentrations from signal intensities. Rare Earth Element abundances were normalized to the Post-Archaean Shale Standard (PAAS) values given in Barth *et al.* (2000).

Ce anomaly (Ce/Ce*) was defined following Noza-ki's (2008) calculation:

$$Ce/Ce^* = 2Ce_N/(La_N + Pr_N) \qquad (1)$$

where 'N' stands for shale-normalized concentration.

For uranium isotope analysis, sample powder was drilled from fresh carbonate sample surfaces with focus on mainly automicrite (for terminology see Hueter *et al.* 2019), as observed and identified during thin-section and SEM analysis. All eleven samples for U isotope analysis were weighted before digestion. For the carbonates, about 600 mg up to 1 g was digested with 6 M HCL in 15 ml Savillex beakers on a hot plate at 100°C and dried overnight. Afterwards, samples were treated with 10 ml of 1.5 M $HNO_3$ and centrifuged after 15 min at ultrasonic bath. The residue was quantitatively transferred into 90 ml Savillex beakers, treated with a mixture of 800 µl conc. $HNO_3$ and 3 ml conc. HCL (*aqua regia*), boiled up at 120°C for 2 hours and evaporated afterwards. All samples were dissolved in 2–5 ml of 3 M $HNO_3$ and subsequently spiked prior to chemical separation of U from the matrix with the IRMM 3636-A ($^{236}U/^{233}U = 0.98130$) mixed isotopic tracer in order to correct for any isotope fractionation on the column as well as instrumental mass bias of the MC-ICP-MS (Weyer *et al.* 2008; Romaniello *et al.* 2013; Noordmann *et al.* 2015).

Uranium separation from the host sample matrix was performed by chromatographical extraction, using Eichrom UTEVA resin (Horwitz *et al.* 1993; Weyer *et al.* 2008). Uranium isotope analyses were performed with a ThermoScientific Neptune Mass Collector-Inductively Coupled Plasma-Mass Spectrometer (MC-ICP-MS) at the Leibniz University Hannover, Germany. Analyses were performed using a Cetac Aridus II combined with a 100 µl PFA nebulizer for sample introduction and a standard Ni sampler cone and a Ni X skimmer cone. With this setup, a 50 ppb U solution was sufficient to achieve a 36 V signal on $^{238}U$ (Weyer *et al.* 2008; Noordmann *et al.* 2015). Every sample was measured three times and results represent mean values (2s.d. typically below 0.1‰). All U isotope variations are reported relative to the U isotopic composition of the CRM112a standard. The results of the isotope measurements are provided in the delta notation:

$$\delta^{238}U \text{ in } ‰$$
$$= \left[ \left(^{238}U/^{235}U\right)_{sample} / \left(^{238}U/^{235}U\right)_{standard-1} \right] \times 1000$$

The U enrichment factors ($U_{EF}$) were calculated to evaluate the terrigenous influence on the U isotope ratios in terms of a detritus correction, using the following notation:

$$U_{EF} = (U/Al)_{sample}/(U/Al)_{standard} \qquad (3)$$

As standard U concentration, the mean concentration of the continental crust (1.3 ppm; Rudnick & Gao 2003) was used. For the standard Al, the continental crust concentration of 83.000 ppm (Greenwood & Earnshaw 1997) was used.

The lanthanum anomaly (La anomaly) was calculated following the established protocol of Bau & Dulski (1996), to test whether the Ce anomaly values are genuine or an artefact caused by elevated or depleted amounts of lanthanum. The calculation of Pr/Pr* is given by $2Pr_N/(Ce_N + Nd_N)$. The calculation of Ce/Ce* is explained in the LA-ICP-MS chapter. For the La anomaly, Ce/Ce* and Pr/Pr* are plotted against each other.

The yttrium/holmium (Y/Ho) ratio was calculated using the element concentrations of the LA-ICP-MS measurements. This ratio acts as an indicator for terrigenous contamination, where ratios close to 30 indicate contamination and ratios around 60 indicate normal seawater signals (Bau & Dulski 1999; Chen *et al.* 2015).

## Results

### Facies characteristics

The fossil assemblage of the Ericeira section studied here (Fig. 3) includes the remains of oysters, echinoderms (crinoids, spines and ossicles), caprinid rudists, madreporite corals, benthic foraminifers (*Palorbitolina lenticularis*, *Neotrocholina*, *Eopalorbitolina*, *Sabaudia minuta*, *Choffatella*, *Lenticulina*, *Everticylammina* sp., *Charentia cuvillieri* and *Meandrospira*) and abundant *L. aggregatum*. Refer to Figures 2 and 3 for an overview of the stratigraphical distribution of skeletal remains based on semi-quantitative thin-section analysis. In order to simplify the description, the succession is divided into three main stratigraphical intervals with different facies associations: (1) lower normal marine facies (0 to 2.5 m); (2) *L. aggregatum* facies (2.5 to 6.1 m); and (3) upper normal marine facies (6.1 to 8.5 m).

*Lower normal marine facies.* – The lowermost part of the section (0–0.7 m) is composed of moderately bioturbated bioclastic grainstones containing abundant bivalve and gastropod shell fragments and occasionally orbitolinid tests. Two prominent, ~20 cm thick, orbitolinid packstone layers are present at section metres 0.4 and 0.7 (Figs 2, 4B). In the overlying

pack- to grainstone interval (0.7–1.4 m), the degree of bioturbation increases significantly. At section metre 1.4, a karstified bedding plane with isolated madreporite corals is present (Fig. 4A, C). There, abundant *Thalassinoides* burrows occur and are often filled with a fine-grained orbitolinid packstone. The strongly bioturbated interval is followed by a 0.7 m thick rudist- and foraminifera-rich grainstone bed (1.5–2.2 m). Slightly above (at 2.3 m), the first nodular *L. aggregatum* occurrence is observed, with individual nodules around 1 cm in diameter. These rocks are also composed of rudist-, bivalve- and foraminifera-rich grainstones up to section metre 2.5.

L. aggregatum facies. – Between section metre 2.5–2.75, *L. aggregatum* oncoids increase in abundance and size, reaching up to 2 cm in diameter. Stratigraphically further upsection, patchy *L. aggregatum* morphotypes (2.8–3.4 m) embedded in higher-energy floatstones are found. This interval is furthermore characterized by abundant cm- to dm-sized, *L. aggregatum* oncoids often with ameboidal morphologies. Intercalated individual madreporite corals are preserved *in situ* and reach up to 15 cm in diameter. Between section metres 3.4 to 4.4, *L. aggregatum* boundstone facies with isolated occurrences of dm-sized corals in growth position encrusted by *L. aggregatum* is present. This microencruster boundstone facies evolves gradually, with increasing abundance of *L. aggregatum* upwards. Furthermore, scattered pockets filled with peloidal orbitolinid grainstone and other benthic foraminifera are common. The dominant growth forms of *L. aggregatum* are cm- to dm-sized flat patchy fabrics. Section metres 4.4 to 4.8 are characterized by the presence of *L. aggregatum* pinnacles (Fig. 4D, 4E). Thin sections reveal the typical cauliflower-like growth morphologies (diameters of 1–20 cm) expanding both up- and sideward. The microencruster network shows mm-thin ferrous–manganese crusts (Fig. 5A) and is surrounded by a poorly consolidated partly dolomitized (Fe-rich) limestone matrix (Fig. 4E) (often) bearing abundant orbitolinids. Occasionally, corals serve as substrates for the formation of *L. aggregatum* crusts. These display well-defined layers, partly with micrite-, and sparite-filled internal cavities. Crusts of *L. aggregatum*, as well as other biogenic components are pervasively bored by lithophage bivalves (*Gastrochaenolites*), endolithic sponges (*Entobia*) and other, taxonomically poorly constrained, microborers. The highest abundance of automicrite facies is present in the pinnacle interval (Fig. 5A/C). Nevertheless, facies containing patches of automicrite is also present beneath and above the intervals dominated by *L. aggregatum*, but is volumetrically less

significant. Above the pinnacle interval (4.8–6.1 m), *L. aggregatum* oncoids are more complex and often irregular, showing ameboidal fabric growth forms (Fig. 2). In this part of the section, the skeletal remains of biomineralizing marine organisms are scarce.

*Upper normal marine facies.* – At 6.1 m, a hiatal surface marks a change in biofacies (6.1–7.1 m; coral lagoon facies) characterized by the return of abundant corals and orbitolinids, as well as minor volumes of bivalves and echinoderm fragments (spines and ossicles). Madreporite corals in life position (Fig. 4F; 6.4 m) are hemispherical and massive, with diameters ranging from 20 to 30 cm. The lithofacies is a coarse orbitolinid-rich pack- to grainstone. Between section metres 7.1 and 7.6, higher-energy packstones to floatstones with rudists, corals, bivalves and benthic foraminifera are present, as well as microbial facies in the form of *L. aggregatum* oncoids forming a volumetrically subordinate component of the rocks. Carbonates in section metres 7.6–8.5 are classified as coral lagoon facies with abundant echinoderms (7.7–7.8 m), madreporite corals in life position and minor occurrences of *L. aggregatum* (8–8.5 m). Dimensions of the madreporite corals gradually decrease (8–8.5 m) upsection. A regional unconformity separates the Ericeira section at its upper boundary from siliciclastic deposits of the Albian Rodízio Formation, heralding the transition towards continental conditions.

## Rare Earth elements (REEs)

Values of Ce anomaly range between 0.8 and 1.0 (Fig. 6A) throughout the Ericeira section. The Ce anomaly values are gradually decreasing from the base to the top of the section. The pinnacle interval (4.4–4.8 m) does not show any significant variation with regard to Ce/Ce* values. The Y/Ho ratios, considered an indicator for terrigenous influence, displays values between 25 and 45, with a clustering near ratios of 35 (Fig. 6B). The La anomaly diagram places most samples in field IIa, a feature that indicates a positive La anomaly resulting in an apparent negative Ce anomaly (Fig. 6C).

The concentration of all REEs ranges between 0 and 4 ppm, and their patterns show low variability. Samples from the lower normal marine facies (0–1.5 m; ER 1, ER 2 and ER 3) display a prominent europium (Eu) anomaly, whereas a lanthanum (La) anomaly, as typical for modern seawater, is absent. The ratio of Light Rare Earth Elements (LREEs) *versus* Heavy Rare Earth Elements (HREEs) is close to 1.0 (Fig. 6D). Overall, the patterns show a 'bell
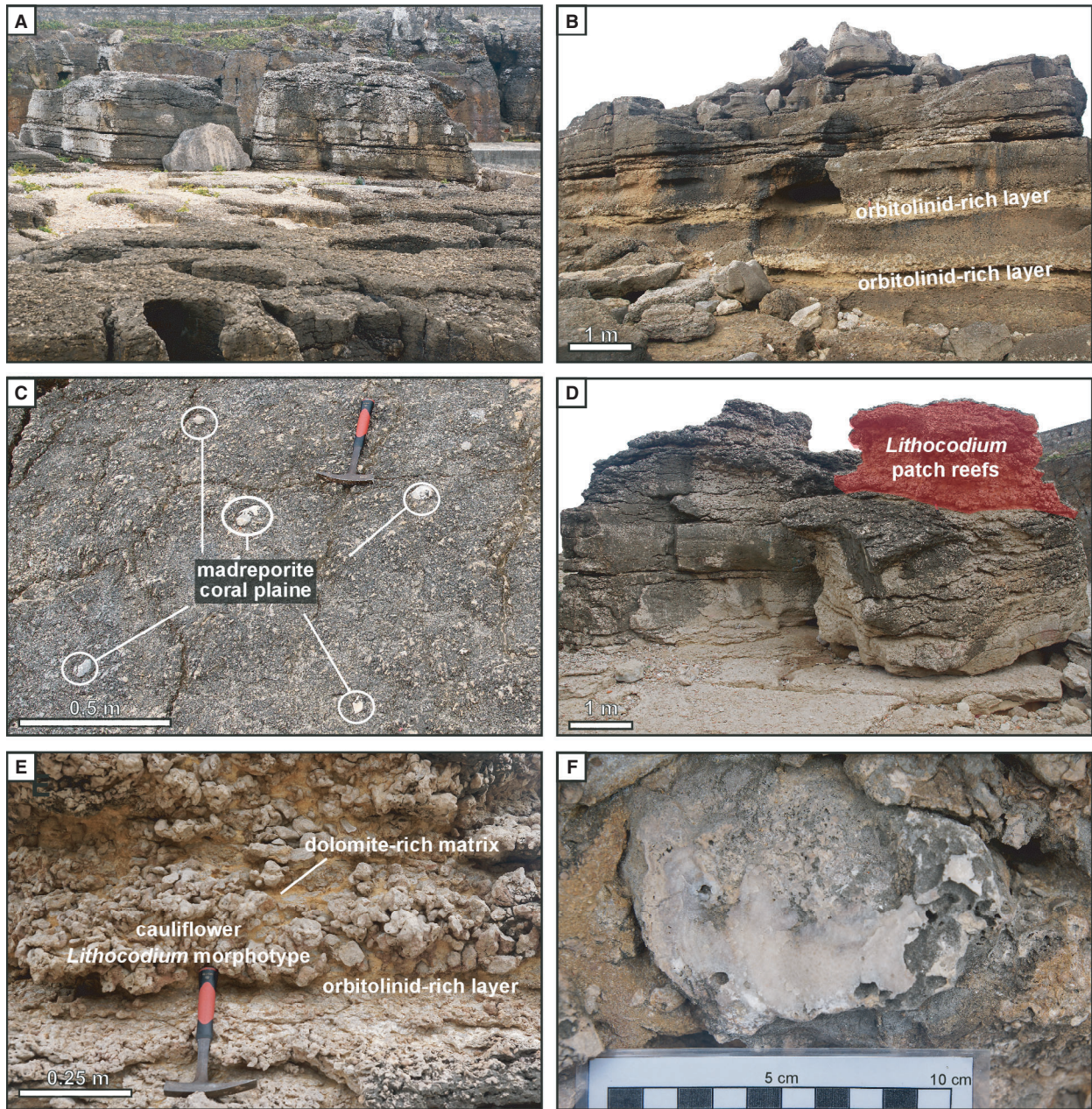
*Fig. 4.* Field images from the Ericeira section. A, overview of the lower part of the succession, karstified bedding plane in the foreground corresponds to section metre 1.4. B, orbitolinid-rich layers at 0.4 and 0.7 m. C, bedding plane showing isolated madreporite corals (section metre 1.4). D, coastal block (section metres 1.4–4.8), including parts of the microencruster interval (pinnacle interval: red colour). E, close-up of *L. aggregatum* of the pinnacle interval (4.4–4.5 m). F, dome-shaped madreporite coral from above the pinnacle interval (at 6.4 m).

shape', most prominent for the samples with the highest Eu anomaly. The concentrations of La, Ce and Pr are rather similar in all samples; therefore, the Ce anomalies are very low or below analytical precision.

## Uranium isotopes

From the base of the Ericeira section, to section metre 1.2, $\delta^{238}U$ values of −0.2 to −0.3 ‰ are observed (Fig. 7A), that is values that are slightly enriched in $^{238}U$ relative to modern seawater (~−0.4 ‰; Weyer *et al.* 2008). Further upsection, a peak value of −0.1 ‰ (metre 1.5) is found. From this interval upsection, values are gradually decreasing to −0.7 ‰ up to section metre 3.3. Upsection, the $\delta^{238}U$ values increase and reach values of −0.3 ‰ at section metre 5.3. From section metre 5.3–7.4 (the stratigraphically uppermost bed), the values remain constant and are slightly enriched in the heavy isotope relative to modern seawater (Fig. 7A).
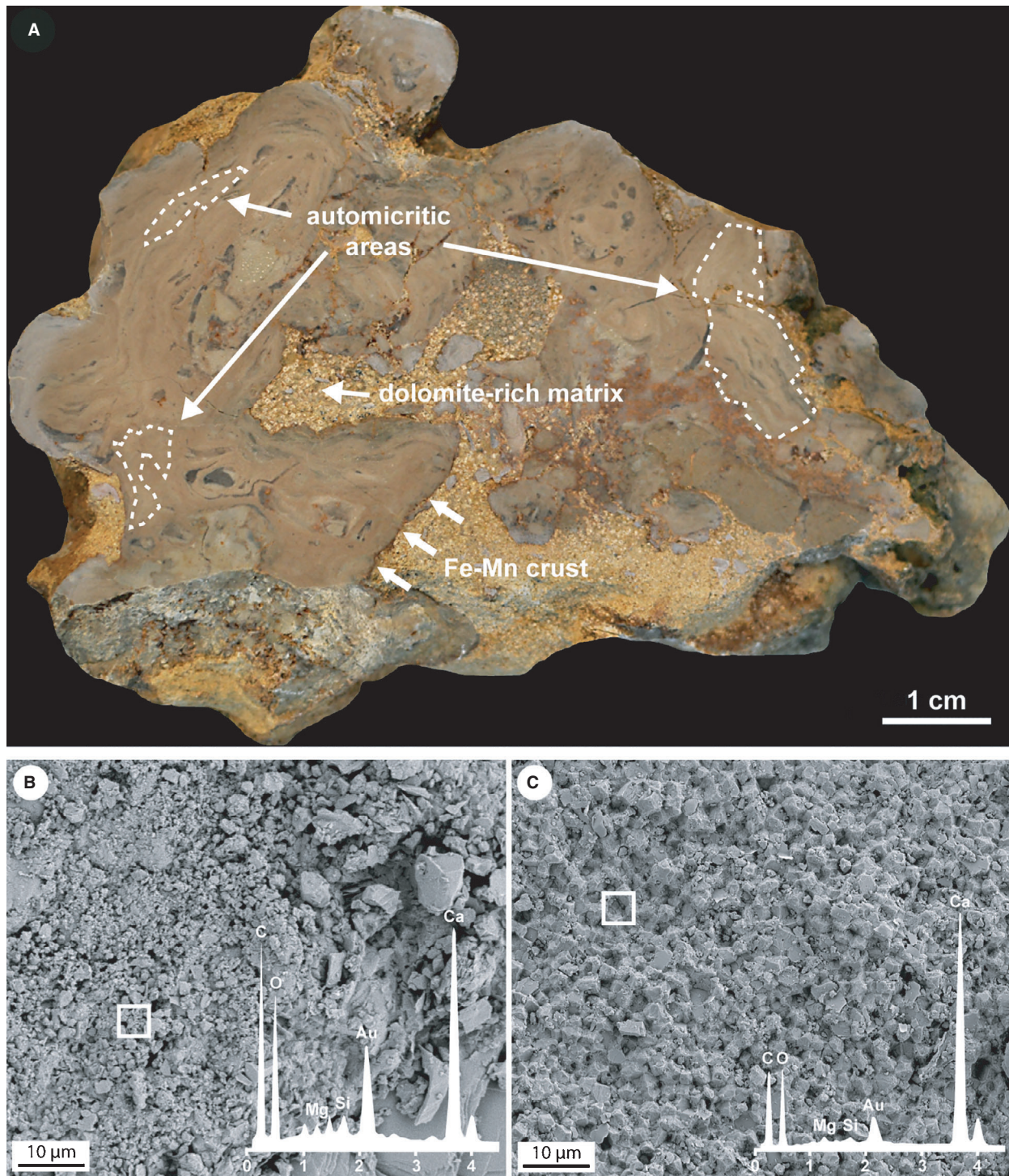
*Fig. 5.* A, polished slab from the pinnacle interval (4.8 m) with prominent reddish ferrous–manganese crusts around the outermost *L. aggregatum* surface, a dolomite-rich matrix and high portions auf automicritic (bright areas within the microencruster layers) material (image from Huck *et al.*2012). B, SEM images of detrital micrite from slightly below the pinnacle interval (3.4 m). C, well-sorted homogenous automicrite from the pinnacle interval (4.7 m) with according energy-dispersive spectroscopy (EDS) element composition data (B, C; lower right).

Uranium concentrations show a very similar pattern (Fig. 7B). Highest U concentrations are observed in the lowermost section metre and again between section metres 5.3 and 6.5, with concentrations of 0.8 up to 1.3 ppm. In the interval with the most negative $\delta^{238}U$ values, concentrations are lowest, ranging between 0.35 and 0.6 ppm.
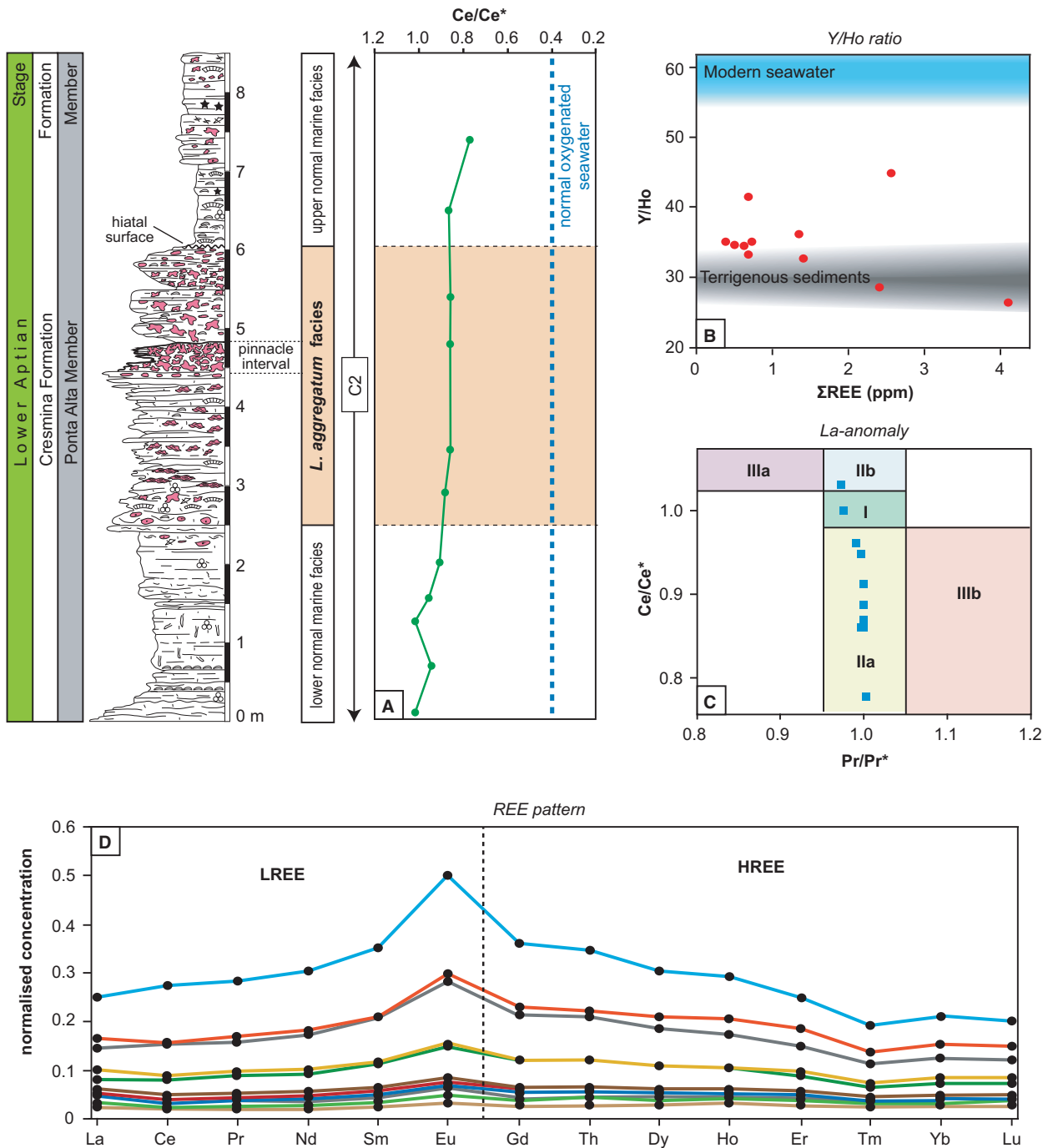
*Fig. 6.* Simplified log of the Ericeira section, with the Ce anomalies. A, Y/Ho ratios to evaluate the terrigenous influence. B, the La anomaly diagram to prove the genuineness of Ce anomalies (C), and Rare Earth Element patterns of the Ericeira section (D), to check for a marine origin for a marine, or a typical 'bell-shaped' pattern for a non-marine signal.

The U enrichment factors ($U_{EF}$) are not correlated with U concentrations (Fig. 7C). Below the pinnacle interval (0 to 4.4 m), the $U_{EF}$ range between 8 and 46, followed by an increase to a maximum of 79 within the pinnacle interval. The U enrichment factors then decrease to values close to 10 until section

metre 6.5. For the uppermost sample (above the pinnacle interval; 7.4 m), the value increases and reaches a value of 46.

Plotting U/Al ratios (ppm/%) *versus* $\delta^{238}U$ values, the outcome reveals that most samples with an $\delta^{238}U$ value close to modern seawater

display U/Al ratios close to 5. In contrast, the sample with the most negative $\delta^{238}U$ value (ER 7; 3.4 m) reflects the highest U/Al ratio close to 15 (Fig. 7D). Furthermore, when plotting U concentration against the $\delta^{238}U$ values (Fig. 7E) samples with the most negative $\delta^{238}U$ values yield the lowest U concentrations and *vice versa*.
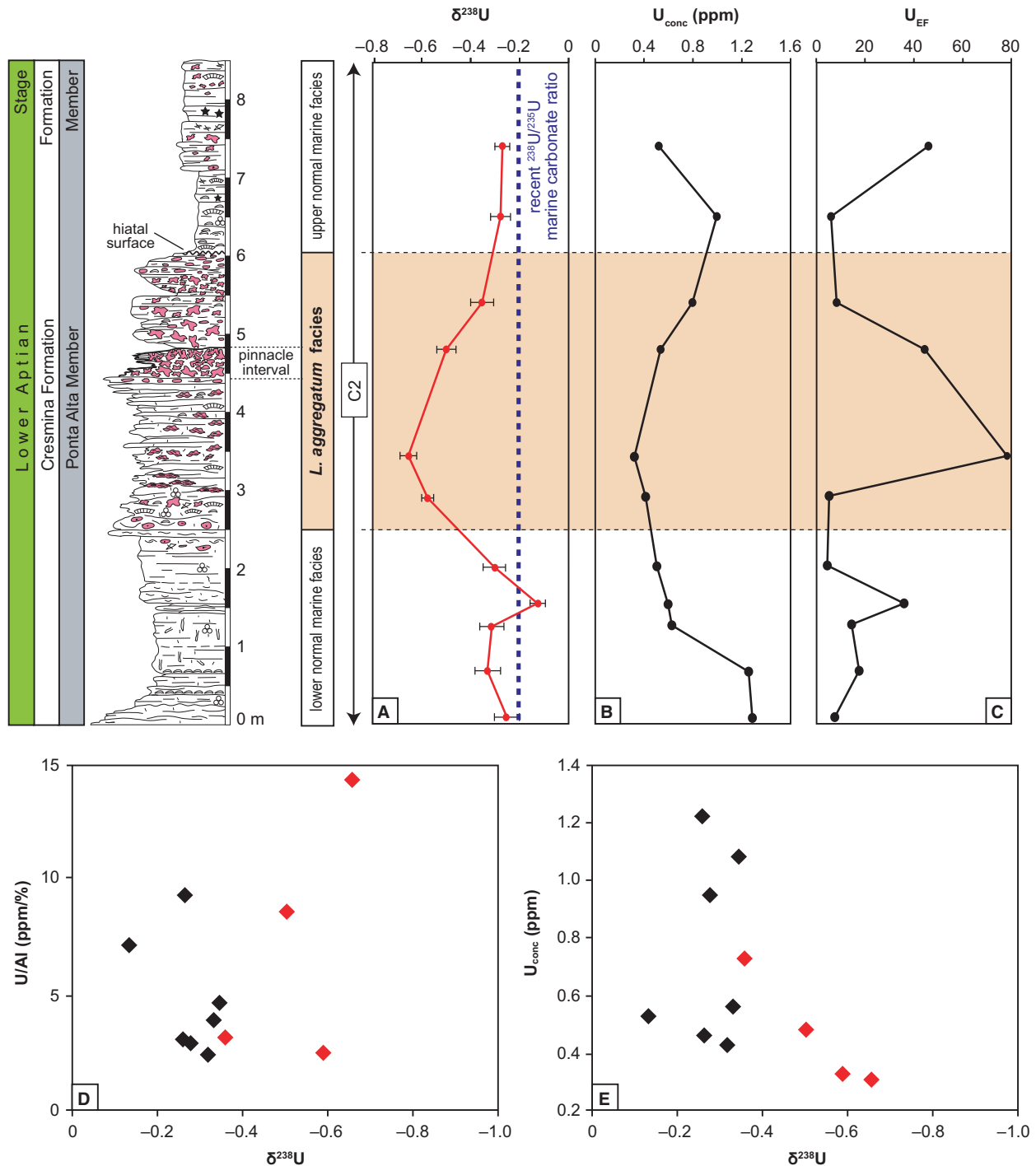


*Fig. 7.* Simplified Ericeira section with $\delta^{238}U$ values (‰). A, displaying values close to modern marine carbonate, throughout the complete section, the U concentration, (B), the U enrichment factors to check for detrital influence on U isotopes (C), and U/Al (ppm/%) against $\delta^{238}U$ (‰) (D), as well as U concentration (ppm) against $\delta^{238}U$ (‰) (E) to exclude any correlation. Samples within the microencruster-dominated interval are marked with red colour (D, E).

# Interpretation and discussion

## Origin and microtexture of fine-grained carbonates

Automicrite, that is fine-grained, autochthonous carbonate with a homogeneous, equigranular nature is usually related to some form of mineral precipitation in biofilms or microbial mats (Neuweiler & Reitner 1992). The former presence of microbial mats or biofilms in fossil microbialites is documented by the layered nature forming crusts of automicrite that might be gravity-defying (Turpin *et al.* 2012, 2014). Microbial films or mats thicken until the supply of nutrients required for cell replication and/or extracellular polymeric substances (EPS) formation becomes critically low. Exopolymeric substances is an umbrella term that groups a wide range of biopolymers (Decho & Kawaguchi 1999). The biotic and abiotic degradation and alteration of EPS favours carbonate precipitation (Dupraz & Visscher 2005). In the case of active precipitation, EPS degradation can increase the alkalinity via liberation of $Ca^{2+}$ ions previously bond to polymers (Reid *et al.* 2000). Passive precipitation within biofilms may take place when the cation binding capacity limit is reached. In this case, the combination of local alkalinity levels and the availability of free $Ca^{2+}$ ions can lead to a spontaneous nucleation of $CaCO_3$ on the EPS matrix (Reid *et al.* 2003).

Automicrites are the materials of choice for the geochemical analyses applied here as the autochthonous, often mono-mineralic nature of these carbonates (Fig. 5C) can be established and proxy data have a high potential to represent the local seawater/marine pore water properties. In contrast, fine-grained detrital carbonate (Fig. 5B) is often a transported material with individual particles displaying variable geochemical signatures typifying a variety of biogenic and abiogenic sources (Turpin *et al.* 2012, 2014). Hence, detrital fine-grained carbonate was not further considered here.

## Oxygen depletion: strategies of recent marine organisms and application to palaeoecology

Many marine organisms have developed strategies to cope with hypoxic conditions. Studies dealing with recent settings document that many organisms are able to detect decreasing dissolved oxygen concentrations on a molecular level (Wu 2002). Pending that these organisms are highly mobile (e.g. fish or portunid crabs), these biotas move into shallower settings to find more oxygen-rich waters and to escape the oxygen-depleted bottom water layer (Breitburg 1992; Wu 2002; Ekau *et al.* 2009). Less mobile species, such as lobsters and echinoderms, crawl to the top of structures rising above the seafloor to avoid hypoxic to anoxic bottom waters (Burd & Brinkhurst 1984). Some echinoderms are known to temporarily change their metabolism to an anaerobic mode, enabling them to survive transient periods of severe hypoxia (Vaquer-Sunyer & Duarte 2008). Burrowing organisms (e.g. worms and shrimp) will emerge onto the sediment surface to escape the rising anoxic horizon (Baden *et al.* 1990; Nilsson & Rosenberg 1994).

With respect to sessile organisms such as for example bivalves, these are able to change their body posture – at least to some degree – to reach higher into the water column by extending their siphon (Jørgensen 1980). Another strategy is to increase the water flow over respiratory structures and to maintain the flux of oxygen by increased ventilation and pumping rates (Warren 1984; Petersen & Petersen 1990). This is, however, coupled with a higher-energy demand and exerts significant stress. Some species reduce their energy demand by either slowing down their metabolic activity, reducing locomotion or increasing the efficiency of metabolic processes (Gracey *et al.* 2001). In general, specific responses to hypoxia are dependent on the remaining oxygen concentration and the duration of oxygen depletion (Vaquer-Sunyer & Duarte 2008), as well as the presence of several previous periods of hypoxia (Altieri 2006).

With reference to Cretaceous oceans, Hueter *et al.* (2019) studied the lower Aptian Kanfanar shallow-water carbonate platform section in Istria (Croatia) characterized by a biological turnover that shares many similarities with that observed in the Ericeira section discusses here. In the Kanfanar section, normal marine biota such as benthic foraminifera, bivalves, gastropods and corals decline significantly in abundance or disappear during an interval dominated by the microencrusting organisms *B. irregularis* and *L. aggregatum*. Hueter *et al.* (2019) demonstrated that platform-top hypoxic water masses triggered this biological turnover, albeit in a depositional setting (isolated platform lacking siliciclastic influx) that differed from the Ericeira one in several aspects.

As a starting point, the presence of a diverse normal marine fauna, as documented from the Ericeira section, is here taken as an indicator of normal oxygenated seawater. The abundance of orbitolinids and other benthic foraminifera, bivalves, corals, echinoderms and gastropods in the lower normal marine facies (0–4.4 m) implies well-oxygenated waters. This observation is supported by pervasive *Thalassinoides*

bioturbation (section metre 0.75–1.4 m; Fig. 2), indicating an oxygenated upper sediment layer (Wetzel 1991; Bromley 1996). The presence of *Thalassinoides* is also in agreement with the coarse and carbonate-rich sediments (0.75–1.4 m) typifying the restricted lagoonal facies, deposited under low sedimentation rates (Löwemark *et al.* 2004).

In the Lusitanian Basin, the first occurrence of *L. aggregatum* (2.25–3.2 m; Fig. 2) is accompanied by a significant decrease in bioturbation, here interpreted as a withdrawal of bioturbating organisms to the sediment surface, and therefore the upward movement of the redox boundary layer to the sediment–water interface (Baden *et al.* 1990; Nilsson & Rosenberg 1994). The prominent *L. aggregatum* mass occurrence as reflected by the pinnacle interval is characterized by a dense packaging of cauliflower growth forms often encrusting coral substrates. The presence of corals, organisms that are bound to normal oxygenated seawater conditions (Laboy-Nieves *et al.* 2001), even within the *L. aggregatum* dominated facies, is indicating variations in the prevailing dissolved oxygen concentrations that control the distribution of organisms. Generally, a decrease in the abundance and diversity of normal marine biota is observed whereas endolithic bivalves (*Gastrochaenolites)* with diameters of <1 cm and boring galleries of sponges (*Entobia*) are still abundant (Huck *et al.* 2012).

An interesting feature is that cavities in the pinnacle architecture are filled with (often dolomitized) orbitolinid wackestones and packstones. Orbitolinids are organisms that are assumed to require normal marine seawater oxygen levels. Nevertheless, it is of importance that the pinnacle interval laterally grades into orbitolinid packstones (São Julião; ~3 km South of Ericeira). Given the winnowed nature of foraminifera in these cavities, it seems likely that they represent hydrodynamically transported fossil assemblages (Huck *et al.* 2012). Several interpretations seem likely.

Orbitolinid-rich sediments formed in more proximal settings that were not affected by whatever environmental parameters triggering the microencruster facies at the study site and were occasionally washed in during storms. These might include more distal, deeper, or coastal environments exposed to more vigorous water circulation. Alternatively, the orbitolinid facies represents slightly older (but not yet consolidated) deposits that formed along the coast prior to the pinnacle intervals. These older sediments were entrained by currents and waves, transported and deposited in cavities of the pinnacle interval. Similar patterns are observed along present-day suboxic coasts and seem rather plausible (Filatoff & Hughes 1996; Nicholas *et al.* 2011; Chen *et al.* 2016).

The pinnacle interval is characterized by conspicuous, mm-thick, reddish to brownish ferrous–manganese crusts coating microencruster surfaces (Fig. 5A). The origin of these crusts allows for multiple interpretations: Generally, the presence of iron and manganese oxide-hydroxides points to abundant dissolved oxygen in the ambient seawater. In modern oceans, manganese- and iron-rich oxide crusts are known from a series of environments that include hydrothermal sources (Toth 1980) in cold pelagic, but also warm, shallow-water environment (Tazaki 2000). Given the coastal setting of the depositional environments investigated here, hydrogenous deposition of metals from a terrigenous source is also a likely interpretation. Examples for these processes are found in the present-day Black Sea where concentration of manganese in seawater takes place under anoxic conditions, is advected towards the redox interface, and then precipitating under oxic conditions (Roy 1992). Trace-element contents in these deposits result from adsorption from seawater onto the iron and manganese colloids during advection. Last but not least, iron and manganese crusts may also form due to clay mineral diagenesis, iron and manganese remobilization, transport and deposition during burial diagenesis (Immenhauser & Rameil 2011).

Important circumstantial evidence is found when taking the orbitolinid sands, filling cavities in the microencruster bindstone fabric, into consideration. Judging from field and thin-section evidence, orbitolinid sands filled cavities after the formation of iron–manganese encrustations and provide clear evidence for a marine origin of these features, that is excluding a late diagenetic origin. Besides the presence of oxygen-dependent corals, the development of Fe–Mn crusts additionally indicates episodes of normal oxygenated seawater. Upsection of the pinnacle interval (4.8–8.5 m), the decrease in the abundance of *L. aggregatum* and the return of bivalves, gastropods, benthic foraminifera and oysters (especially above the transgressive surface at section metre 6.1) documents the return of normal marine oxygenated seawater conditions.

## Geochemical redox proxies applied to modern carbonates: implications for palaeoseawater redox reconstructions

Geochemical redox proxies applied to near-coastal shallow-water carbonates are very helpful tools but, unfortunately, susceptible to several factors other than redox levels (Ling *et al.* 2013). Below we discuss these proxies based on features observed in Recent settings and critically compare these observations

with evidence collected from the Cretaceous section in Portugal. Examples for the complexity of these proxies are found in studies documenting uranium enrichment and $^{238}U/^{235}U$ isotope ratios of Recent organic-rich surface sediments across continental margins (Abshire *et al.* 2020).

*Uranium enrichment and U isotope ratios.* – Uranium has a long seawater residence time (~0.5 Myr; Dunk *et al.* 2002), occurs in two redox states, U (IV) and U (VI) and is rather soluble in oxygenated water due to the predominant uranyl ion $U_{VI}O_2^{2-}$ stabilized by the formation of non-reactive carbonate complexes (Calvert & Pedersen 1993). In suboxic and anoxic environments, the reduction of U (VI) to U (IV) is important for the removal of U from the oceans (Morford & Emerson 1999; McManus *et al.* 2006). Modern seawater has $\delta^{238}U$ values in the order of −0.4‰ (Weyer *et al.* 2008). In any ideal scenario, the $\delta^{238}U$ values of modern primary carbonate precipitates and well-preserved corals (aragonitic) with an age of up to 600 ka are undistinguishable from the $\delta^{238}U$ of modern seawater (Stirling *et al.* 2007; Tissot & Dauphas 2015). Recent bulk carbonate sediments are usually slightly offset from seawater (up to 0.2‰) due to the incorporation of minor amounts of U (IV) into the carbonate lattice (Chen *et al.* 2018). Hence, different carbonate particles within the same sample might display variable $\delta^{238}U$ values (Hood *et al.* 2018). Variations in $\delta^{238}U$ values are further induced by microbial reduction of U (VI) to U (IV) under anoxic conditions at the sediment–water interface (Zheng *et al.* 2002). During the incorporation of U into carbonate precipitated in the upper water column, the U isotope composition will fractionate to heavier values, pending that the seawater is anoxic or hypoxic. In case of an oxic upper water column and anoxic deep-water masses, significant reduction-driven U isotope fractionation takes place (Romaniello *et al.* 2013; Chen *et al.* 2018). Furthermore, terrigenous input can influence the $\delta^{238}U$ signature and samples must be screened for detrital Al concentrations and the $U_{EF}$ must be corrected for a detrital signal.

In the case of the Ericeira carbonates, $\delta^{238}U$ values in the first two section metres are slightly enriched in $^{238}U$ relative to modern seawater. Chen *et al.* (2018), however, proposed that carbonates may indeed show an average offset of about ~0.2 ‰ relative to seawater. Assuming that this offset can be applied to the data shown here, $\delta^{238}U$ values reflect carbonate sediments deposited in oxic seawater with U values of −0.4 ‰ (Fig. 7A). With reference to samples taken from the *Lithocodium* facies, $\delta^{238}U$ values decrease and reach a minimum of −0.7 ‰. Possible

explanations for these, relative to modern seawater, depleted $\delta^{238}U$ values are: (1) a light detrital source of U (Holmden *et al.* 2015) resulting in an incorrect correction for terrigenous U; (2) a U isotope fractionation towards isotopically depleted $\delta^{238}U$ during carbonate deposition; (3) a local source of isotopically light U in a restricted setting; and (4) a globally lower seawater $\delta^{238}U$ at the time of deposition. Given that the Ericeira carbonate section was deposited prior to the onset of OAE 1a, the notion of a globally lower seawater $\delta^{238}U$ signature, expected during the acme of OAE 1a (Brennecka *et al.* 2011), seems unlikely. Moreover, a local source of isotopically light U in a restricted basin, due to the connection to the North Atlantic is equally unlikely. In contrast, iron-rich dolomites and ferrous–manganese crusts, both characteristic features of the pinnacle interval, potentially act as sources of light U during diagenesis and dissolution. The most likely interpretation is perhaps that of a riverine light detrital U source and furthermore, fractionation towards isotopically depleted $\delta^{238}U$ during carbonate deposition.

The U enrichment factors beneath and above the pinnacle interval are generally higher than 5, a feature that suggests only moderate terrigenous influence. Any given value larger than 1.0 points to an enrichment relative to the average crustal abundance. Enrichment factors >3 represent a statistically relevant enrichment, and values >10 represent a moderate to strong degree of enrichment (Algeo & Tribovillard 2009).

In modern normal marine systems, enrichment of U in sediments can be classified as follows: (1) oxic environments are typified by a minor enrichment; (2) suboxic environments typically display a moderate enrichment ($U_{EF} < 10$); and (3) anoxic environments show characteristically high levels of enrichments ($U_{EF} > 10$; Algeo & Tribovillard 2009; Abshire *et al.* 2020). Two samples taken from the here studied microencruster interval provide $U_{EF}$ values that are significantly higher (45 to 80) (section metres 3.4 and 4.8; Fig. 7C), which might therefore point to anoxic conditions. The high $U_{EF}$ values could be consistent with the low $\delta^{238}U$ and the low U concentration of seawater, if assuming a global expansion of seafloor anoxia. In case of a fast development of anoxia, U becomes more non-conservative and features a shorter ocean residence time, allowing a change of seawater $\delta^{238}U$ at time scales of 10 k.y. (Brennecka *et al.* 2011; Lau *et al.* 2016; Elrick *et al.* 2017). Nevertheless, regarding the pre-OAE 1a setting studied here, a fast global expansion of seafloor anoxia is unlikely.

Summing up, for the interpretation of an anoxic setting (similar to the Kanfanar section, Croatia;

Hueter *et al.* 2019), the most pronounced seawater oxygen depletion and the most prominent peak in the $\delta^{238}U$ values in the Ericeira section would be expected in the microencruster-dominated facies (2.5–6.1 m) and especially within section metres 4.4 and 4.8 (pinnacle interval). In the Ericeira section, this $\delta^{238}U$ peak (−0.7‰) is present at section metre 3.4 (Fig. 7A), that is below the pinnacle interval. Furthermore, the $\delta^{238}U$ values return to 'normal oxidized seawater' U values within the microencruster-dominated facies and below the hiatal surface (6.1 m). In an anoxic environment, such a return to normal values would be likely found above the microencruster-dominated facies, given that a change in facies and biota is an indicator for a change in seawater redox conditions (trend to more oxygenated conditions). Given the long residence time of U in seawater (~0.5 Myr; Dunk *et al.* 2002), short-term patterns recorded here do not reflect the U isotope composition of seawater. Given the pre-OAE 1a age of this section, it therefore seems more plausible that iron-rich dolomites and Fe–Mn crusts acted as source of light U or, even more likely, riverine input acted as light U source and caused a fractionation towards isotopically depleted U during the carbonate deposition. This interpretation is in agreement with the extremely high $U_{EF}$ ($U_{EF} > 10$ indicate substantial authigenic enrichment; Algeo & Tribovillard 2009) suggesting terrigenous influence (connection to the hinterland) as controlling factor for the U isotopic signal (same for REEs), rather than genuine changes in seawater redox conditions.

*Rare Earth Elements and cerium anomaly.* – Rare Earth Elements and specifically Ce anomalies are among the most widely applied redox proxies (German *et al.* 1991; Sholkovitz & Schneider 1991; Bellanca *et al.* 1997; Bodin *et al.* 2013; Della Porta *et al.* 2015). Cerium, present in its tetravalent state in oxic environments will be preferentially removed from the water column by scavenging processes. In open marine, oxidized environments, Ce oxidation is mediated through bacterial activity and takes place in the upper oceanic water masses. Hence, Ce anomalies serve as tracers of palaeoredox conditions in the upper water column. When these water masses become anoxic, Ce turns to its reduced state and behaves chemically similar to its neighbours La and Pr. Specifically, the Ce/Ce* ratio tends then to be closer to 1.

As material of choice for the palaeoredox reconstruction with Ce anomalies, microbial automicrite has been proven to record the ambient seawater REE geochemistry and can serve as a tracer of palaeooxygen levels (Olivier & Boyet 2006; Della Porta *et al.*

2015). Analysis requires comparably large sample volumes (0.5–1 g), a prerequisite that is given in samples taken from the microbial crusts associated with the pinnacle interval (Fig. 5C). Care must be taken to not combine data from automicrites and such from detrital micrite. This issue was circumvented by comparing the Si content of detrital micrite and automicrite in EDS spectra (Guido *et al.* 2011). Pinnacle interval automicrites display very low Si contents providing support to the notion as *in situ*, non-detrital materials (Fig. 5B, C).

Moreover, the concentration of specific REEs has a direct influence on the Ce anomaly values. This is because the Ce anomaly is calculated from the concentration differences of La, Ce and Pr. To exclude this bias, the La anomaly diagram of Bau & Dulski (1996) is commonly applied (Fig. 6C). In the case of the Ericeira section, most values plot in field IIa of Figure 6, indicating a positive La anomaly. The implication of this is that the Ce pattern observed in the Portugal section is the product of an anomaly in La, and therefore does not reflect a true depletion in the seawater oxygen content.

REE concentrations behave comparably conservative during diagenesis (Nothdurft *et al.* 2004) whereas Ce anomalies are susceptible to a variety of influences (Sholkovitz & Shen 1995) including: terrigenous influence, high aluminium (Al) and scandium (Sc) concentrations, and anomalies in lanthanum concentrations. Ling *et al.* (2013) place an upper Al concentration limit at 0.35 % (3500 ppm) and at 2 ppm for Sc. In the Ericeira section, the concentrations of both elements are significantly lower (Al ≤ 1500 and Sc ≤ 1 ppm). Moreover, REE patterns measured in the Portugal section (Fig. 6D) take up the typical 'bell-shaped' pattern, interpreted as an indicator for contamination and/or riverine influence (Della Porta *et al.* 2015). This interpretation is supported by the LREEs to HREEs ratio, which is close to, or even above 1.

The yttrium/holmium (Y/Ho) ratio is a widely used screening tool to detect terrigenous contamination (Fig. 6B). Chen *et al.* (2015) place the minimum Y/Ho value of seawater signal at 35. Modern seawater Y/Ho ratios are close to 60 or higher whereas values of 35 or lower must be treated with care and most likely reflect contamination. Y/Ho ratios measured in samples taken from the Ericeira section range between 25 and 45 (mean of 35), a feature that points to a pronounced terrigenous influence.

Summing up, the Ce anomalies observed in the Portugal section suggests that this proxy is biased by terrigenous influence (La anomaly), a notion that seems likely in these coastal sections, and should not be used as evidence for seawater anoxia. Uranium

isotopes represent the most intricate proxy but suggest well-oxygenated conditions, close to the recent $\delta^{238}U$ values, throughout the section studied. Minor variations of the $\delta^{238}U$ values can be explained by local changes in seawater redox conditions and do not reflect strong oxygen-depleted conditions. Therefore, proxy data must be handled with care and oxygen depletion seems unlikely.

## How to deal with conflicting palaeoecological and geochemical evidence?

Assessing the above-discussed geochemical data from the Portugal section, oxygen-depleted seawater as main stressor driving the transient decline of a diverse marine fauna and the rise of the microencruster buildup facies seems unlikely. This outcome stands in clear contrast to data documented in Hueter *et al.* (2019) from a Central Tethyan shallow-water setting, showing evidence for a correlation between oxygen-depleted platform-top water masses and the transient mass occurrence of (bacinelloid) microencrusters. Clearly, the response of Cretaceous carbonate platform ecosystems to environmental change is complex and might be regionally and temporally different even where similar facies patterns are observed.

Following Schmitt *et al.* (2019), we tentatively suggest that a combination of several stressors induced the palaeoecological trends observed. Previous authors (Immenhauser *et al.* 2005; Waite *et al.* 2007; Rameil *et al.* 2010; Schlagintweit *et al.* 2010; Bover-Arnal *et al.* 2011; Huck *et al.* 2012) argued that increased trophic levels and water-quality decline (algal bloom and turbid waters) are relevant factors to be considered. In the (relatively proximal) coastal Ericeira section, due to its connection to the hinterland, an increase in riverine run-off and nutrient availability is likely and documented in the geochemical proxies applied here. Furthermore, high-amplitude relative sea-level fluctuations, resulting from the opening of the proto-North Atlantic (Rey *et al.* 2003; Dinis *et al.* 2008) might have played a role.

Observations from Recent nearshore sediment-impacted reefal systems might be, at least to some degree, relevant in this context. Many classical studies suggested that sediment particles and related nutrient influx smother reefal organisms, stunt and kills corals and reduces illumination relevant for photosynthesis (Rodgers 1990). Lokier *et al.* (2009) demonstrated the presence of a clear relationship between the volume of siliciclastic/volcanoclastic sediment input and the composition and nature of carbonate-producing organisms. On the other hand, it has been demonstrated that some sessile reefal organisms tolerate short-term burial and can survive in high-energy environments where strong currents or wave activity exhumes sediment-covered organisms (Larcombe & Woolfe 1999; Wolanski *et al.* 2005). Despite the ability of many sessile benthic organisms to clear small amounts of sediment from their surfaces (Rodgers 1983; Rosen *et al.* 2002; Lirman & Manzello 2009), becoming temporarily covered by sediments is still a major stressor and potentially lethal, either due to a reduced efficient photosynthesis or because of physically blocked feeding mechanisms (Woolfe & Larcombe 1999). With references to Holocene scleractinian coral reefs, significant sediment and nutrient input into the reefal domain is related to a reduced species number, less live corals, lower growth rates and decreased calcification, greater abundance of branching forms, reduced coral recruitment and slower rates of reef accretion (Rodgers 1990; Erftemeijer *et al.* 2012; Jones *et al.* 2015). The presence of turbid, nutrient-rich waters, however, does not mean that coral growth is entirely prohibited and a somewhat more refined view has been proposed in more recent work (Lokier *et al.* 2009; Perry *et al.* 2009, 2012; Ryan *et al.* 2016; Santodomingo *et al.* 2016; Johnson *et al.* 2017). In some cases, suboptimal habitats are now considered as important in their role of reefal diversification by hosting a pool of species tolerant to stressed conditions (Ryan *et al.* 2016; Santodomingo *et al.* 2016). Evidence suggests the existence of well-developed Holocene reefs with high accretion rates in turbid shallow-water habitats, characterized by high sedimentation rates and siliciclastic input (Perry *et al.* 2009, 2012; Ryan *et al.* 2016). It is proposed that studies documenting the response of Recent nearshore reefal ecosystems to water-quality decline might form an interesting starting point for future work. For the time being, and with reference to the Cretaceous case example studied here, we conclude that we find no evidence that significant amounts of (transient) clastic influx suffocated the coral–rudist facies in the Ericeira section, and by this created an ecological niche that was subsequently occupied by microencruster facies. Hence, if patterns in clastic influx and, related to this, trophic levels, were significant factors in the Cretaceous case study discussed here, then amount of clastic influx was not comparable with that of sediment-impacted reefs as described from the modern world. Nevertheless, we consider the lessons from the Recent basically meaningful, and suggest that they should form a starting point for future research aiming at a better understanding of these fossil faunal turnover events.

# Conclusions

This study documents, compares and discusses a palaeoecological and a geochemical data set across a conspicuous upper Barremian–lower Aptian shallow-marine carbonate platform succession in Portugal. The most prominent feature in the section studied is the decline of what is considered a normal marine rudist–coral ecosystem and the transient establishment of a microencruster facies forming metre-sized, morphologically complex buildups. Geochemical palaeoredox proxies (Ce/Ce* and $\delta^{238}U$ isotope data) are applied to autochthonous microbial (auto)micrite samples collected from this section in order to assess the significance of changes in dissolved seawater oxygen levels (coastal anoxia). The outcome documents the complexity of these proxies applied to nearshore shallow-marine sediments. Chemostratigraphical anomalies in Ce/Ce* ratios are observed, but likely reflect terrigenous influence (La anomaly) rather than changes in seawater dissolved oxygen levels. The interpretation of uranium isotope data is not straightforward but suggest well-oxygenated conditions, close to recent seawater $\delta^{238}U$ values, throughout the section studied. Excluding coastal seawater anoxia as main stressor, it seems likely that a set of environmental stressors including perhaps trophic levels and high-frequency relative sea-level change, among other factors, caused the stratigraphical patterns observed in Portugal, a scenario that is in agreement with previous work (Bover-Arnal *et al.* 2011; Huck *et al.* 2012). The outcome of this study contrasts recent work by Hueter *et al.* (2019) documenting a clear relation between Central Tethyan OAE1a-time equivalent microencruster intervals that formed as response to time intervals when shallow-marine seawater anoxia established. Clearly, the interaction of middle Cretaceous carbonate platform ecosystems with environmental stressors and water-quality decline is highly complex. Even when palaeoecological patterns in different sections share important similarities, evidence for directly comparable causal relations is as yet lacking.

## Data availability statement

Data used for this study are available upon request to the corresponding author (alexander.hueter@rub.de).

## References

Abshire, M.L., Romaniello, S.J., Kuzminov, A.M., Cofrancesco, J., Severmann, S. & Riedinger, N. 2020: Uranium isotopes as a proxy for primary depositional redox conditions in organic-rich marine systems. *Earth and Planetary Science Letters 529*, 115878.

Algeo, T.J. & Tribovillard, N. 2009: Environmental analysis of paleoceanographic systems based on molybdenum-uranium covariation. *Chemical Geology 268*, 211–225.

Altieri, A.H. 2006: Inducible variation in hypoxia tolerance across the intertidal-subtidal distribution of the blue mussel *Mytilus edulis*. *Marine Ecology Progress Series 325*, 295–300.

Altieri, A.H. & Diaz, R.J. 2019: Dead zones: oxygen depletion in coastal ecosystems. *In* Sheppard, C. (ed): *World Seas: An Environmental Evaluation (2nd edition), Vol. 3: Ecological Issues and Environmental Impacts*. Academic Press, 453–473.

Alves, T.M., Moita, C., Cunha, T., Ullnaess, M., Myklebust, R., Monteiro, J.H. & Manupella, G. 2009: Diachronous evolution of Late Jurassic-Cretaceous continental rifting in the northeast Atlantic (West Iberian Margin). *Tectonics 28*, TC4003.

Baden, S.P., Loo, L.O., Pihl, L. & Rosenberg, R. 1990: Effects of eutrophication on benthic communities including fish: Swedish west coast. *Ambio 19*, 113–122.

Barth, M.G., McDonough, W.F. & Rudnick, R.L. 2000: Tracking the budget of Nb and Ta in the continental crust. *Chemical Geology 165*, 197–213.

Bau, M. & Dulski, P. 1996: Distribution of yttrium and rare-earth elements in the Penge and Kuruman iron-formations, Transvaal Supergroup, South Africa. *Precambrian Research 79*, 37–55.

Bau, M. & Dulski, P. 1999: Comparing yttrium and rare earths in hydrothermal fluids from the Mid-Atlantic Ridge: implications for Y and REE behaviour during near-vent mixing and for the Y/Ho ratio of Proterozoic seawater. *Chemical Geology 155*, 77–90.

Bellanca, A., Masetti, D. & Neri, R. 1997: Rare earth elements in limestone/marlstone couplets from the Albian-Cenomanian Cismon section (Venetian region, northern Italy): assessing REE sensitivity to environmental changes. *Chemical Geology 141*, 141–152.

Bodin, S., Godet, A., Westermann, S. & Föllmi, K. 2013: Secular change in northwestern Tethyan water-mass oxygenation during the late Hauterivian – early Aptian. *Earth and Planetary Science Letters 374*, 121–131.

Bottini, C., Cohen, A.S., Erba, E., Jenkyns, H.C. & Coe, A.L. 2012: Osmium-isotope evidence for volcanism, weathering, and ocean mixing during the early Aptian OAE 1a. *Geology 40*, 583–586.

Bover-Arnal, T., Salas, R., Martin-Closas, C., Schlagintweit, F. & Moreno-Bedmar, J.A. 2011: Expression of an oceanic anoxic event in a neritic setting: Lower Aptian coral rubble deposits from the western Maestrat Basin (Iberian Chain, Spain). *Palaios 26*, 18–32.

Breitburg, D.L. 1992: Episodic hypoxia in Chesapeake Bay: interacting effects of recruitment, behavior, and physical disturbance. *Ecological Monographs 62*, 525–546.

Brennecka, G.A., Herrmann, A.D., Algeo, T.J. & Anbar, A.D. 2011: Rapid expansion of oceanic anoxia immediately before the end-Permian mass extinction. *Proceedings of the National Academy of Sciences of the USA 108*, 17631–17634.

Bromley, R.G. 1996: *Trace Fossils: Biology, Taphonomy and Applications*, 361 pp. Chapman and Hall, London.

Burd, B.J. & Brinkhurst, R.O. 1984: The distribution of the galatheid crab *Munida quadrispina* (Benedict, 1902) in relation to oxygen concentrations in British Columbia fjords. *Journal of Experimental Marine Biology and Ecology 81*, 1–20.

Burla, S., Heimhofer, U., Hochuli, P.A., Weissert, H. & Skelton, P. 2008: Changes in sedimentary patterns of coastal and deep sea successions from the North Atlantic (Portugal) linked to Early Cretaceous environmental change. *Palaeogeography, Palaeoclimatology, Palaeoecology 257*, 38–57.

Burla, S., Oberli, F., Heimhofer, U., Wiechert, U. & Weissert, H. 2009: Improved time control on Cretaceous coastal deposits: New results from Sr isotope measurements using laser ablation. *Terra Nova 21*, 401–409.

Calvert, S.E. & Pedersen, T.F. 1993: Geochemistry of recent oxic and anoxic marine-sediments - implications for the geological record. *Marine Geology 113*, 67–88.

Chen, C.T.A. 2008: Effects of climate change on marine ecosystems. *In Fisheries for Global Welfare and Environment 5th World Fisheries Congress*, 307–316.

Chen, J., Algeo, T.J., Zhao, L., Chen, Z.-Q., Cao, L., Zhang, L. & Li, Y. 2015: Diagenetic uptake of rare earth elements by bioapatite, with an example from Lower Triassic conodonts of South China. *Earth-Science Reviews 149*, 181–202.

Chen, M., Hongshuai, Q., Dongzhao, L., Binbin, L. & Fang, Q. 2016: Paleoenvironmental Evolution of the Beilun River Estuary, Northwest South China Sea, During the Past 20,000 Years Based on Diatoms. *Acta Geologica Sinica 90*, 2244–2257.

Chen, X., Romaniello, S.J., Herrmann, A.D., Hardisty, D., Gill, B.C. & Anbar, A.D. 2018: Diagenetic effects on uranium isotope fractionation in carbonate sediments from the Bahamas. *Geochimica et Cosmochimica Acta 237*, 294–311.

Coccioni, R., Nesci, O., Tramontana, C.F., Wezel, C.F. & Moretti, E. 1987: Descrizione di un livello guida 'Radiolaritico-Bituminoso-Ittiolitico' alla base delle Marne a Fucoidi nell'Appennino Umbro-Marchigiano. *Bollettino della Società geologica italiana 106*, 183–192.

Da Gama, R.B.P., Bown, P.R. & Cabral, M.C. 2009: Calcareous nannofossil biostratigraphy of an outcrop section of Aptian sediments of west-central Portugal (Lusitanian Basin). *Journal of Micropalaeontology 28*, 153–160.

Decho, A.W. & Kawaguchi, T. 1999: Confocal imaging of in situ natural microbial communities and their extracellular polymeric secretions using nanoplast resin. *BioTechniques 27*, 1246–1252.

Della Porta, G., Webb, G.E. & McDonald, I. 2015: REE patterns of microbial carbonates and cements from Sinemurian (Lower Jurassic) siliceous sponge mounds (Djebel Bou Dahar, High Atlas, Morocco). *Chemical Geology 400*, 65–86.

Diaz, R.J. & Rosenberg, R. 1995: Marine Benthic Hypoxia: A review of its ecological effects and the behavioural responses of benthic macrofauna. *Oceanography and Marine Biology 33*, 245–303.

Diaz, R.J. & Rosenberg, R. 2008: Spreading dead zones and consequences for marine ecosystems. *Science 321*, 926–929.

Dickson, A.J., Cohen, A.S. & Coe, A.L. 2012: Seawater oxygenation during the Paleocene-Eocene Thermal Maximum. *Geology 40*(7), 639–642.

Dinis, J.L., Rey, J., Cunha, P.P., Callapez, P. & Pena dos Reis, R. 2008: Stratigraphy and allogenic controls of the western Portugal Cretaceous: an updated synthesis. *Cretaceous Research 29*, 772–780.

Dunk, R.M., Mills, R.A. & Jenkins, W.J. 2002: A reevaluation of the oceanic uranium budget for the Holocene. *Chemical Geology 190*, 45–67.

Dupraz, C. & Visscher, P.T. 2005: Microbial lithification in marine stromatolites and hypersaline mats. *Trends in Microbiology 13*, 429–438.

Ekau, W., Auel, H., Portner, H.O. & Gilbert, D. 2009: Impacts of hypoxia on the structure and processes in pelagic communities (zooplankton, macro-invertebrates and fish). *Biogeoscience 7*, 1669–1699.

Elrick, M., Polyak, V., Algeo, T.J., Romaniello, S., Asmerom, Y., Herrmann, A.D., Anbar, A.D., Zhao, L. & Chen, Z.-Q. 2017: Global-ocean redox variation during the middle-late Permian through Early Triassic based on uranium isotope and Th/U trends of marine carbonates. *Geology 45*, 163–166.

Erba, E., Bottini, C., Weissert, J.H. & Keller, C.E. 2010: Calcareous nannoplankton response to surface-water acidification around Oceanic Anoxic Event 1a. *Science 329*, 428–432.

Erftemeijer, P.L.A., Riegl, B., Hoeksema, B.W. & Todd, P.A. 2012: Environmental impacts of dredging and other sediments on corals: a review. *Marine Pollution Bulletin 64*, 1737–1765.

Filatoff, J. & Hughes, G.W. 1996: Late Cretaceous to Recent palaeoenvironments of the Saudi Arabian Red Sea. *Journal of African Earth Sciences 22*, 535–548.

Föllmi, K.B., Bodin, S., Godet, A., Linder, P. & van de Schootbrugge, B. 2007: Unlocking paleo-environmental information from Early Cretaceous shelf sediments in the Helvetic Alps: stratigraphy is the key!. *Swiss Journal of Geosciences 100*, 349–369.

Föllmi, K.B., Bôle, M., Jammet, N., Froidevaux, P., Godet, A., Bodin, S., Adatte, T., Matera, V., Fleitmann, D. & Spangenberg, J.E. 2012: Bridging the Faraoni and Selli oceanic anoxic events: late Hauterivian to early Aptian dysaerobic to anaerobic phases in the Tethys. *Climate of the Past 8*, 171–189.

Föllmi, K.B., Godet, A., Bodin, S. & Linder, P. 2006: Interactions between environmental change and shallow water carbonate buildup along the northern Tethyan margin and their impact on the Early Cretaceous carbon isotope record. *Paleoceanography 21*.PA4211.

German, C.R., Holliday, B.P. & Elderfield, H. 1991: Redox cycling or rare earth elements in the suboxic zone of the Black Sea. *Geochimica et Cosmochimica Acta 55*, 3553–3558.

Gracey, A.Y., Troll, J.V. & Somero, G.N. 2001: Hypoxia-induced gene expression profiling in the euryoxic fish *Gillichthys mirabilis*. *Proceedings of the National Academy of Sciences of the USA 98*, 1993–1998.

Greenwood, N.N. & Earnshaw, A. 1997: *Chemistry of the Elements*. 2nd edn. Butherworth-Heineman, Oxford: 1–1342.

Guido, A., Papazzoni, C.A., Mastandrea, A., Morsilli, M., La Russa, M.F., Tosti, F. & Russo, F. 2011: Automicrite in a 'nummulite bank' from the Monte Saraceno (Southern Italy): evidence for synsedimentary cementation. *Sedimentology 58*, 878–889.

Guinotte, J.M. & Fabry, V.J. 2008: Ocean acidification and Its Potential Effects on Marine Ecosystems. *Annals of the New York Academy of Sciences 1134*, 320–342.

Hart, B.T., Lake, P.S., Webb, J.A. & Grace, M.R. 2003: Ecological risk to aquatic systems from salinity increases. *Australian Journal of Botany 51*, 689–702.

Hay, W.W., DeConto, R.M., Wold, C.N., Wilson, K.M., Voigt, S., Schulz, M., Rossby Wold, A., Dullo, W.C., Ronov, A.B., Balukhovsky, A.N. & Söding, E. 1999: Alternative global Cretaceous paleogeography, *In*Barrera, E. & Johnson, C.C. (eds): *Evolution of the Cretaceous Ocean-Climate System*. Geological Society of America Special Paper 332, 1–47.

Heimhofer, U., Hochuli, P.A., Burla, S. & Weissert, H. 2007: New records of Early Cretaceous angiosperm pollen from Portuguese coastal deposits: Implications for the timing of the early angiosperm radiation. *Review of Palaeobotany and Palynology 144*, 39–76.

van Hinsbergen, D.J.J., de Groot, L.V., van Schaik, S.J., Spakman, W., Bijl, P.K., Sluijs, A., Langereis, C.G. & Brinkhui, H. 2015: A paleolatitude calculator for paleoclimate studies (model version 2.1). *PLoS One 10*, e0126946.

Hiscott, R.N., Wilson, R.C.L., Gradstein, F.M., Pujalte, V., Garcia-Mondejar, J., Boudreau, R.R. & Wishart, H.A. 1990: Comparative stratigraphy and subsidence history of Mesozoic rift basins of North-Atlantic. *American Association of Petroleum Geologists Bulletin 74*, 60–76.

Holmden, C., Amini, M. & Francois, R. 2015: Uranium isotope fractionation in Saanich Inlet: A modern analog study of a paleoredox tracer. *Geochimica et Cosmochimica Acta 153*, 202–215.

Hood, A.V.S., Planavsky, N.J., Wallace, M.W. & Wang, X. 2018: The effects of diagenesis on geochemical paleoredox proxies in

sedimentary carbonates. *Geochimica et Cosmochimica Acta* 232, 265–287.

Horwitz, E.P., Chiarizia, R., Dietz, M.L. & Diamond, H. 1993: Separation and preconcentration of actinides from acidic media by extraction chromatography. *Analytica Chimica Acta* 281, 361–372.

Huck, S., Heimhofer, U. & Immenhauser, A. 2012: Early Aptian algal bloom in a neritic proto-North Atlantic setting: Harbinger of global change related to OAE 1a? *Geological Society of America Bulletin* 124, 1810–1825.

Huck, S., Heimhofer, U., Immenhauser, A. & Weissert, H. 2013: Carbon-isotope stratigraphy of Early Cretaceous (Urgonian) shoal-water deposits: Diachronous changes in carbonate-platform production in the north-western Tethys. *Sedimentary Geology* 290, 157–174.

Huck, S., Heimhofer, U., Rameil, N., Bodin, S. & Immenhauser, A. 2011: Strontium and carbon-isotope chronostratigraphy of Barremian-Aptian shoal-water carbonates: Northern Tethyan platform drowning predates OAE 1a. *Earth and Planetary Science Letters* 304, 547–558.

Huck, S., Rameil, N., Korbar, T., Heimhofer, U., Wieczorek, T.D. & Immenhauser, A. 2010: Latitudinally different responses of Tethyan shoal-water carbonate systems to the Early Aptian oceanic anoxic event (OAE 1a). *Sedimentology* 57, 1585–1614.

Huck, S., Stein, M., Immenhauser, A., Skelton, P.W., Christ, N., Föllmi, K.B. & Heimhofer, U. 2014: Response of proto-North Atlantic carbonate-platform ecosystems to OAE1a-related stressors. *Sedimentary Geology* 313, 15–31.

Hueter, A., Huck, S., Bodin, S., Heimhofer, U., Weyer, S., Jochum, K.P. & Immenhauser, A. 2019: Central Tethyan platform-top anoxia during Oceanic Anoxic Event 1a. *Climate of the Past* 15, 1327–1344.

Immenhauser, A., Hillgärtner, H. & van Bentum, E. 2005: Microbial-foraminiferal episodes in the early Aptian of the southern Tethyan margin: Ecological significance and possible relation to oceanic anoxic event 1a. *Sedimentology* 52, 77–99.

Immenhauser, A. & Rameil, N. 2011: Interpretation of ancient epikarst features in carbonate successions - a note of caution. *Sedimentary Geology 239*, 1–9.

Jenkyns, H.C. 2010: Geochemistry of oceanic anoxic events. *Geochemistry, Geophysics, Geosystems 11*, Q03004.

Johnson, J.A., Perry, C.T., Smithers, S.G., Morgan, K.M., Santodomingo, N. & Johnson, K.G. 2017: Palaeoecological records of coral community development on a turbid, nearshore reef complex: baselines for assessing ecological change. *Coral Reefs* 36, 685–700.

Jones, N.S., Ridgwell, A. & Hendy, E.J. 2015: Evaluation of coral reef carbonate production models at a global scale. *Biogeosciences 12*, 1339–1356.

Jørgensen, B.B. 1980: Seasonal oxygen depletion in the bottom waters of a Danish fjord and its effects on the benthic community. *Oikos 34*, 68–76.

Kirwan, M.L., Guntenspergen, G.R., D'Alpaos, A., Morris, J.T., Mudd, S.M. & Temmerman, S. 2010: Limits on the adaptability of coastal marshes to rising sea level. *Geophysical Research Letters 37*, L23401.

Laboy-Nieves, E.N., Klein, E., Conde, J.E., Losada, F., Cruz, J.J. & Bone, D. 2001: Mass mortality of tropical marine communities in Morrocoy, Venezuela. *Bulletin of Marine Science 68*, 163–179.

Larcombe, P. & Woolfe, K.J. 1999: Increased sediment supply to the Great Barrier Reef will not increase sediment accumulation at most coral reefs. *Coral Reefs 18*, 163–169.

Lau, K.V., Maher, K., Altiner, D., Kelley, B.M., Kump, L.R., Lehrmann, D.J., Silva-Tamayo, J.C., Weaver, K.L., Yu, M. & Payne, J.L. 2016: Marine anoxia and delayed Earth system recovery after the end-Permian extinction. *Proceedings of the National Academy of Sciences of the USA 113*, 2360–2365.

Leinfelder, R.R., Nose, M., Schmid, D.U. & Werner, W. 1993: Microbial Crusts of the Late Jurassic: Composition, palaeoecological significance and importance in reef construction. *Facies 29*, 195–230.

Levin, L.A., Ekau, W., Gooday, A.J., Jorissen, F., Middelburg, J.J., Naqvi, S.W.A., Neira, C., Rabalais, N.N. & Zhang, J. 2009: Effects of natural and human-induced hypoxia on coastal benthos. *Biogeosciences 6*, 2063–2098.

Ling, H.-F., Chen, X., Li, D., Wang, D., Shields-Zhou, G.A. & Zhu, M. 2013: Cerium anomaly variations in Ediacaran-earliest Cambrian carbonates from the Yangtze Gorges area, South China: Implications for oxygenation of coeval shallow seawater. *Precambrian Research 225*, 110–127.

Lirman, D. & Manzello, D. 2009: Patterns of resistance and resilience of the stress-tolerant coral *Siderastrea radians* (Pallas) to sub-optimal salinity and sediment burial. *Journal of Experimental Marine Biology and Ecology 369*, 72–77.

Lokier, S.W., Wilson, M.E.J. & Burton, L.M. 2009: Marine biota response to clastic sediment influx: A quantitative approach. *Palaeogeography, Palaeoclimatology, Palaeoecology 281*, 25–42.

Löwemark, L., Schönfeld, J., Werner, F. & Schäfer, P. 2004: Trace fossils as a paleoceanographic tool: evidence from Late Quaternary sediments of the southwestern Iberian margin. *Marine Geology 204*, 27–41.

Masse, J.P. & Chartrousse, A. 1997: Les Caprina (Rudistes) de l'Aptien inférieur d'Europe occidentale; systématique, biostratigraphie et paléobiogéographie. *Geobios 30*, 797–809.

McManus, J., Berelson, W.M., Severmann, S., Poulson, R.L., Hammond, D.E., Klinkhammer, G.P. & Holm, C. 2006: Molybdenum and uranium geochemistry in continental margin sediments: Paleoproxy potential. *Geochimica et Cosmochimica Acta 70*, 4643–4662.

Morford, J.L. & Emerson, S. 1999: The geochemistry of redox sensitive trace metals in sediments. *Geochimica et Cosmochimica Acta 63*, 1735–1750.

Neuweiler, F. & Reitner, J. 1992: Karbonatbänke mit Lithocodium aggregatum ELLIOTT / Bacinella irregularis RADOICIC. *Berliner geowissenschaftliche Abhandlungen 3*, 273–293.

Nicholas, W.A., Chivas, A.R., Murray-Wallace, C.V. & Fink, D. 2011: Prompt transgression and gradual salinization of the Black Sea during the early Holocene constrained by amino acid racemization and radiocarbon dating. *Quaternary Science Reviews 30*, 3769–3790.

Nielsen, D.L., Brock, M.A., Rees, G.N. & Baldwin, D.S. 2003: Effects of increasing salinity on freshwater ecosystems in Australia. *Australian Journal of Botany 51*, 655–665.

Nilsson, H.C. & Rosenberg, R. 1994: Hypoxic response of two marine benthic communities. *Marine Ecology Progress Series 115*, 209–217.

Noordmann, J., Weyer, S., Montoya-Pino, C., Dellwig, O., Neubert, N., Eckert, S., Paetzel, M. & Böttcher, M.E. 2015: Uranium and molybdenum isotope systematics in modern euxinic basins: Case studies from the central Baltic Sea and the Kyllaren fjord (Norway). *Chemical Geology 396*, 182–195.

Nothdurft, L.D., Webb, G.E. & Kamber, B.S. 2004: Rare earth element geochemistry of Late Devonian reefal carbonates, Canning Basin Western Australia: confirmation of a seawater REE proxy in ancient limestones. *Geochimica et Cosmochimica Acta 68*, 263–283.

Nozaki, Y.2008: Rare Earth Elements and their isotopes in the Ocean. *In*Steele, J.H., Turekian, K.K. & Thorpe, S.A. (eds): *Encyclopedia of Ocean Sciences* (2nd edn), 653–665.

Olivier, N. & Boyet, M. 2006: Rare earth and trace elements of microbialites in Upper Jurassic coral- and sponge-microbialite reefs. *Chemical Geology 230*, 105–123.

Perry, C.T., Smithers, S.G., Gulliver, P. & Browne, N.K. 2012: Evidence of very rapid reef accretion and reef growth under high turbidity and terrigenous sedimentation. *Geology 40*, 719–722.

Perry, C.T., Smithers, S.G. & Johnson, K.G. 2009: Long-term coral community records from Lugger Shoal on the terrigenous inner-shelf of the central Great Barrier Reef, Australia. *Coral Reefs 28*, 941–948.

Petersen, J.K. & Petersen, G.I. 1990: Tolerance, behavior and oxygen consumption in the sand goby, *Pomatoschistus minutus* (Pallus), exposed to hypoxia. *Journal of Fish Biology 37*, 921–933.

Rabalais, N.N., Diaz, R.J., Levin, L.A., Turner, R.E., Gilbert, D. & Zhang, J. 2010: Dynamics and distribution of natural and human-caused hypoxia. *Biogeosciences 7*, 585–619.

Rabalais, N.N. & Turner, R.E. 2001: Hypoxia in the Northern Gulf of Mexico: description, causes and change, in: Coastal and estuarine studies: coastal hypoxia consequences for living resources and ecosystems. *In* Rabalais, N.N. & Turner, R.E. (eds): *American Geophysical Union*, 1–36. Washington, D.C.

Rameil, N., Immenhauser, A., Warrlich, G., Hillgärtner, H. & Droste, H.J. 2010: Morphological patterns of Aptian *Lithoco-dium-Bacinella* geobodies: relation to environment and scale. *Sedimentology 57*, 883–911.

Rasmussen, E.S., Lomholt, S., Andersen, C. & Vejbæk, O.V. 1998: Aspects of the structural evolution of the Lusitanian Basin in Portugal and the shelf and slope area offshore Portugal. *Tectonophysics 300*, 199–225.

Reid, R.P., James, N.P., Macintyre, I.G., Dupraz, C.P. & Burne, R.V. 2003: Shark Bay stromatolites: Microfabrics and reinterpretation of origins. *Facies 49*, 299–324.

Reid, R.P., Visscher, P.T., Decho, A.W., Stolz, J.F., Bebout, B.M., Dupraz, C., Macintyre, I.G., Paerl, H.W., Pinckney, J.L., Prufert-Bebout, L., Steppe, T.F. & DesMarais, D.J. 2000: The role of microbes in accretion, lamination and early lithification of modern marine stromatolites. *Nature 406*, 989–992.

Rey, J., de Graciansky, P.C. & Jaquin, T. 2003: Les sequences de dépôt dans le Crétacé inférieur du Bassin Lusitanien. *Comunicaçoes do Instituto Geológico e Mineiro 90*, 15–42.

Robinson, S.A., Heimhofer, U., Hesselbo, S.P. & Rose Petrizzo, M. 2017: Mesozoic climates and oceans – a tribute to Hugh Jenkyns and Helmut Weissert. *Sedimentology 64*, 1–15.

Rodgers, C.S. 1983: Sublethal and lethal effects of sediments applied to common Caribbean reef corals in the field. *Marine Pollution Bulletin 14*, 378–382.

Rodgers, C.S. 1990: Responses of coral reefs and reef organisms to sedimentation. *Marine Ecology Progress Series 62*, 185–202.

Romaniello, S.J., Herrmann, A.D. & Anbar, A.D. 2013: Uranium concentrations and $^{238}U/^{235}U$ isotope ratios in modern carbonates from the Bahamas: Assessing a novel paleoredox proxy. *Chemical Geology 362*, 305–316.

Rosen, B.R., Aillud, G.S., Bosellini, F.R., Clack, N.J. & Insalaco, E. 2002: Platy coral assemblages: 200 million years of functional stability in response to the limiting effects of light and turbidity. *In Proceedings of the 9th International Coral Reef Symposium* volume *1*, 255–264.

Roy, S. 1992: Environments and Processes of Manganese Deposition. *Economic Geology 87*, 1218–1236.

Rudnick, R.L. & Gao, S. 2003: Composition of the continental crust. *Treatise on Geochemistry 3*, 1–64.

Ryan, E.J., Smithers, S.G., Lewis, S.E., Clark, T.R. & Zhao, J.X. 2016: Chronostratigraphy of Bramston Reef reveals a long-term record of fringing reef growth under muddy conditions in the central Great Barrier Reef. *Palaeogeography, Palaeoclimatology, Palaeoecology 441*, 734–747.

Santodomingo, N., Renema, W. & Johnson, K.G. 2016: Understanding the murky history of the Coral Triangle: Miocene corals and reef habitats in East Kalimantan (Indonesia). *Coral Reefs 35*, 765–781.

Schlagintweit, F., Bover-Arnal, T. & Salas, R. 2010: New insights into *Lithocodium aggregatum* Elliott 1956 and *Bacinella irregularis* Radoičić 1959 (Late Jurassic-Lower Cretaceous): two ulvophycean green algae (?Order Ulotrichales) with a heteromorphic life cycle (epilithic/euendolithic). *Facies 56*, 509–547.

Schlanger, S.O. & Jenkyns, H.C. 1976: Cretaceous oceanic anoxic events: Causes and consequences. *Geologie en Mijnbouw 55*, 179–184.

Schmitt, K., Heimhofer, U., Frijia, G. & Huck, S. 2019: Platform-wide shift to microbial carbonate production during the late Aptian. *Geology 47*, 786–790.

Sholkovitz, E.R. & Schneider, D.L. 1991: Cerium redox cycles and rare earth elements in the Sargasso Sea. *Geochimica et Cosmochimica Acta 55*, 2737–2743.

Sholkovitz, E. & Shen, G.T. 1995: The incorporation of rare-earth elements in modern coral. *Geochimica et Cosmochimica Acta 59*, 2749–2756.

Skelton, P.W. & Masse, J.-P. 1998: Revision of the Lower Cretaceous rudistgenera *Pachytraga Paquier* and *Retha Cox* (Bivalvia: Hippuritacea), and the origins of the Caprinidae. *Geobios 31*, 331–370.

Smith, V.G., Joye, S.B. & Howarth, R.W. 2006: Eutrophication of freshwater and marine ecosystems. *Limnology and Oceanography 51*, 351–355.

Stirling, C.H., Andersen, M.B., Potter, E.K. & Halliday, A.N. 2007: Low-temperatures isotopic fractionation of uranium. *Earth and Planetary Science Letters 264*, 208–225.

Tazaki, K. 2000: Formation of banded iron-manganese structures by natural microbial communities. *Clays and Clay Minerals 48*, 511–520.

Tissot, F.L.H. & Dauphas, N. 2015: Uranium isotopic compositions of the crust and ocean: age corrections, U budget and global extent of modern anoxic. *Geochimica et Cosmochimica Acta 167*, 113–143.

Tostevin, R., Wood, R.A., Shields, G.A., Poulton, S.W., Guilbaud, R., Bowyer, F., Penny, A.M., He, T., Curtis, A., Hoffmann, K.H. & Clarkson, M.O. 2016: Low-oxygen waters limited habitable space for early animals. *Nature Communications 7*, 12818.

Toth, J.R. 1980: Deposition of submarine crusts rich in manganese and iron. *Geological Society of America Bulletin 91*, 44–54.

Turpin, M., Emmanuel, L., Immenhauser, A. & Renard, M. 2012: Geochemical and petrographical characterization of fine-grained carbonate particles along proximal to distal transects. *Sedimentary Geology 281*, 1–20.

Turpin, M., Gressier, V., Bahamonde, J.R. & Immenhauser, A. 2014: Component-specific petrographic and geochemical characterization of fine-grained carbonate along Carboniferous and Jurassic platform-to-basin transects. *Sedimentary Geology 300*, 62–85.

Vaquer-Sunyer, R. & Duarte, C.M. 2008: Thresholds of hypoxia for marine biodiversity. *Proceedings of the National Academy of Sciences 105*, 15452–15457.

Waite, L.E., Scott, R.W. & Kerans, C. 2007: Middle Albian age of the regional dense marker bed of the Edwards Group, Pawnee Field, south-central Texas. *Gulf Coast Association of Geological Societies Transactions 57*, 759–774.

Warren, L.M. 1984: How intertidal polychaetes survive at low tide. *In* Hutchings, P.A. (ed.):. *Proceedings of the First International Polychaete Conference*, 238–253.

Weissert, H., Lini, A., Föllmi, K.B. & Kuhn, O. 1998: Correlation of Early Cretaceous carbon isotope stratigraphy and platform drowning events: a possible link? *Palaeogeography, Palaeoclimatology, Palaeoecology 137*, 189–203.

Wetzel, A. 1991: Ecologic interpretation of deep-sea trace fossil communities. *Palaeogeography, Palaeoclimatology, Palaeoecology 85*, 47–69.

Weyer, S., Anbar, A.D., Gerdes, A., Gordon, G.W., Algeo, T.J. & Boyle, E.A. 2008: Natural fractionation of $^{238}U/^{235}U$. *Geochimica et Cosmochimica Acta 72*, 345–359.

Wilson, R.C.L., Hiscott, R.N., Willis, M.G. & Gradstein, F.M. 1989: The Lusitanian Basin of west-central Portugal: Mesozoic and Tertiary tectonic, stratigraphic, and subsidence history. *In* Tankard, A.J. & Balkwill, H.R. (eds): *Extensional Tectonics and Stratigraphy of the North Atlantic Margins*, 341–361. American Association of Petroleum Geologists Memoir.

Wolanski, E., Fabricius, K., Spagnol, S. & Brinkman, R. 2005: Fine sediment budget on an inner-shelf coral-fringed island, Great Barrier Reef of Australia. *Estuarine, Coastal and Shelf Science 65*, 153–158.

Woolfe, K.J. & Larcombe, P. 1999: Terrigenous sedimentation and coral reef growth: a conceptual framework. *Marine Geology 155*, 331–345.

Wu, R.S.S. 2002: Hypoxia: from molecular responses to ecosystem responses. *Marine Pollution Bulletin 45*, 35–45.

Zheng, Y., Anderson, R.F., van Green, A. & Fleischer, M.Q. 2002: Preservation of non-lithogenic particulate uranium in marine sediments. *Geochimica et Cosmochimica Acta 66*, 3085–3092.